POLITECNICO DI TORINO
Repository ISTITUZIONALE

Neotectonic study of the Western Crete and implications for seismic hazard assessment

Original
Neotectonic study of the Western Crete and implications for seismic hazard assessment / Mountrakis, D.; Kilias, A.; Pavlaki, A.; Fassoulas, C.; Thomaidou, E.; Papazachos, C.; Papaioannou, C.; Roumelioti, Z.; Benetatos, Christoforos; Vamvakaris, D.. - In: JOURNAL OF THE VIRTUAL EXPLORER. - ISSN 1441-8142. - ELETTRONICO. - 42:(2012). [10.3809/jvirtex.2011.00285]

Availability:
This version is available at: 11583/2500022 since: 2022-04-27T14:06:07Z

Publisher:
Australian Crustal Research Centre

Published
DOI:10.3809/jvirtex.2011.00285

Terms of use:

This article is made available under terms and conditions as specified in the corresponding bibliographic description in the repository

Publisher copyright

(Article begins on next page)

26 April 2025

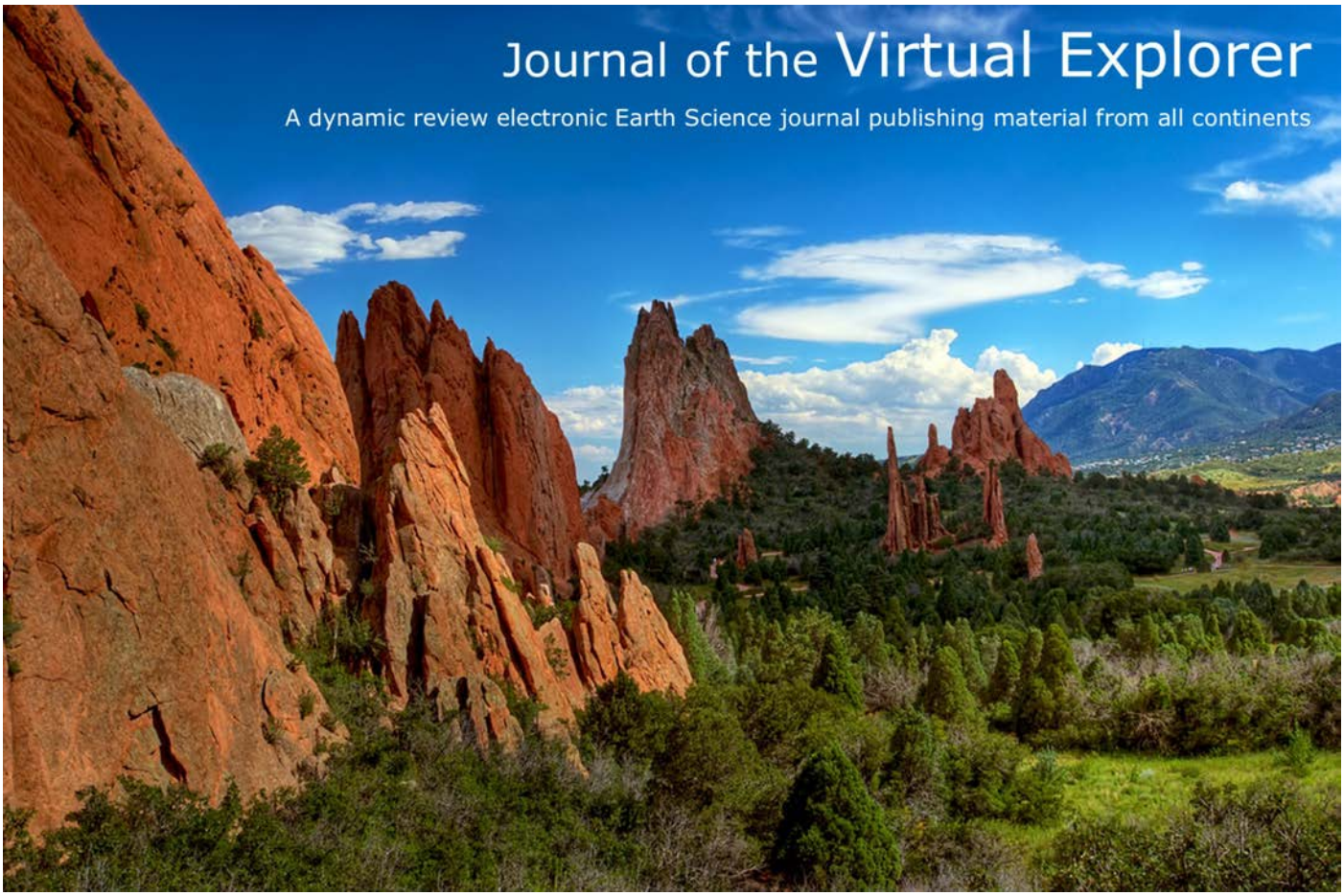

Neotectonic study of Western Crete and implications for seismic hazard assessment

Demosthenis Mountrakis, A. Kilias, A. Pavlaki, C. Fassoulas, E. Thomaidou, C. Papazachos, C. Papaioannou, Z. Roumelioti, et al

Journal of the Virtual Explorer, Electronic Edition, ISSN 1441-8142, volume **42**, paper 2
In: (Eds.) Emmanuel Skourtsos and Gordon S. Lister, The Geology of Greece, 2012.

Download from: http://virtualexplorer.com.au/article/2011/285/neotectonic-study-of-western-crete

Click http://virtualexplorer.com.au/subscribe/ to subscribe to the Journal of the Virtual Explorer.
Email team@virtualexplorer.com.au to contact a member of the Virtual Explorer team.

Copyright is shared by The Virtual Explorer Pty Ltd with authors of individual contributions. Individual authors may use a single figure and/or a table and/or a brief paragraph or two of text in a subsequent work, provided this work is of a scientific nature, and intended for use in a learned journal, book or other peer reviewed publication. Copies of this article may be made in unlimited numbers for use in a classroom, to further education and science. The Virtual Explorer Pty Ltd is a scientific publisher and intends that appropriate professional standards be met in any of its publications.

Journal of the Virtual Explorer, 2012
Volume 42
Paper 2
http://virtualexplorer.com.au/

Neotectonic study of Western Crete and implications for seismic hazard assessment

Demosthenis Mountrakis
Aristotle University of Thessaloniki, Department of Geology.*Email: dmountra@geo.auth.gr*

A. Kilias
Aristotle University of Thessaloniki, Department of Geology.

A. Pavlaki
Aristotle University of Thessaloniki, Department of Geology.

C. Fassoulas
University of Crete, Natural History Museum of Heraklion.

E. Thomaidou
Aristotle University of Thessaloniki, Department of Geology.

C. Papazachos
Aristotle University of Thessaloniki, Department of Geophysics.

C. Papaioannou
Institute of Engineering Seismology and Earthquake Engineering.

Z. Roumelioti
Aristotle University of Thessaloniki, Department of Geophysics.

C. Benetatos
Aristotle University of Thessaloniki, Department of Geophysics.

D. Vamvakaris
Aristotle University of Thessaloniki, Department of Geophysics.

Abstract: A detailed study has been realized in the framework of a large-scale seismotectonic survey in Western Crete (Southern Greece), for the creation of a revised neotectonic map in a scale of 1:50.000, including the recognition and mapping of the main neotectonic faults and the evaluation of their seismic potential. For this reason, the faults under investigation were distinguished as active, possible active and inactive. Kinematic data and striations were used to estimate the corresponding stress field geometry. Two distinctive stress phases were recognized, operating after the Middle Miocene extensional exhumation of deep crustal rocks. The first N-S extension phase (D_1) took place during Mid-Upper Miocene to Lower Pliocene, forming large normal faults, trending mainly E-W, that bound the large Neogene basins. The second phase (D_2) took place during late Pliocene-Quaternary times, forming medium-to-large normal faults that trend mainly N-S, related to an E-W extension. In the E-W trending D_1 faults, a younger strike-slip striation usually occurs, compatible with the later D_2 kinematics. Smaller, mainly NE-SW trending faults, with significant lateral displacement, indicate a kinematic compatibility to the more recent D_2 phase. Some of these faults act as transfer zones between the larger N-S trending D_2 faults. Considering the fault length and the using several geological criteria for their seismic risk evaluation, we recognized 13 large major fault zones in the study area, six of which were considered as active, while three as possible active faults. Results obtained from the analysis of fault plane solution information verify both the determined active (D_2 phase) stress field results, as well as the local kinematic behavior of the neotectonic faulting. Moreover, a detailed seismic hazard analysis, involving both probabilistic and deterministic approaches, shows a significant spatial variation of the various hazard measures, with the seismic hazard of the westernmost part of study area being controlled by the neighboring higher seismicity neotectonic faults.

Citation: 2012. Neotectonic study of Western Crete and implications for seismic hazard assessment. In: (Eds.) Emmanuel Skourtsos and Gordon S. Lister, *Journal of the Virtual Explorer*, volume **42**, paper 2, doi: 10.3809/jvirtex.2011.00285

Introduction

The study area of Western Crete is located in the Southern Aegean subduction zone, which includes the outer Subduction Arc (Crete, Peloponnesus, Rhodes, etc.) and the inner Volcanic Arc (fig 1). The seismotectonic features of the broader Southern Aegean area are controlled by the presence of a complex subduction of the Eastern Mediterranean lithosphere beneath the Aegean Sea lithosphere, as well as the interaction of the Aegean, Anatolia and Eastern Mediterranean lithospheres (e.g. Papazachos and Comninakis, 1970, McKenzie, 1970, 1972, Le Pichon and Angelier, 1979). This complicated geodynamic interaction has imprinted itself on the observed geological and seismotectonic setting. A typical example is the presence of different types of stress-regimes and corresponding faulting, often with spatial overlapping (e.g. Papazachos *et al.*, 1998), including: a) Large thrust submarine faults located along the outer Hellenic arc (e.g. south western part of Crete) due to the NE-SW convergence compression, b) Medium N-S trending normal faults, located either on land or along the western and eastern borders Crete, Karpathos and southern Peloponnesus due to an arc-parallel E-W extension field, c) Large-to-medium E-W trending normal faults throughout the main part of the Aegean Sea and the Greek and Turkey mainland, corresponding to a roughly N-S trending extension and, d) Right and left-lateral strike-slip faults along the broader Kefalonia and Rhodes area, respectively, defining the external borders of the Aegean lithosphere, which exhibits a SW plate motion of the order of 35mm/yr with respect to stable Eurasia (Oral *et al.*, 1995, Reilinger *et al.*, 1997, Papazachos, 1999, McClusky *et al.*, 2000). Moreover, a well developed Benioff zone is observed (e.g. Papazachos *et al.*, 2000), with medium-to-large transpressional intermediate-depth events, mainly occurring in the depth range of 60-90km, with maximum depths of the order of 180km. The subduction is associated with an active Volcanic Arc (e.g. Fytikas *et al.*, 1984), with the volcanic centre of Santorini in Central Cyclades, being the most active volcano of the area.

The island of Crete is situated in a fore-arc position above the active northward-directed subduction zone of the African plate beneath the Aegean plate (Petereck and Schwarze 2004). Crete is a structurally complicated area (fig. 2, 3), been strongly affected by the Alpine orogenic processes in Eastern Mediterranean from Jurassic to present day, due to plate convergence of Eurasian and African plates and the subduction of the Tethyan oceanic crust (Bonneau 1984, Lister *et al.*, 1984, Mountrakis 2006, Ring *et al.*, 2010, Kilias *et al.*, 2010). Nappes stacking and compression alternate with extension, nappes collapse and exhumation of deep crustal rocks (fig. 3; Bonneau 1976, 1984, Seidel *et al.*, 1982, Kilias *et al.*, 1994, 2002, Jolivet *et al.*, 1996).

The convergence of Eurasian and African plates in Eastern Mediterranean region and the subduction of the later beneath the former in the Hellenic arc from Late Oligocene until now, resulted in the intense neotectonics and active deformation in Aegean area, in Crete and in the whole internal Hellenic region (Kilias *et al.* 1994, Jolivet *et al.*, 1996, ten Veen & Kleinspehn 2003). This deformation is displayed as continuous expansion and thinning of the Aegean crust (Goldworthy *et al.*, 2002) and is revealed by the creation of new, as well as the reactivation of older major faults, which are responsible for the formation or reorientation of large Neogene - Quaternary troughs. This active deformation is also presently manifested by the occurrence of strong shallow earthquakes along the Hellenic Arc, including the broader area of Crete. In general, the largest seismicity levels are observed along the outer Hellenic arc (south of Crete), within the NE-SW compression zone due to the Aegean-Eastern Mediterranean convergence (fig. 1). A typical case is the major Elafonisos fault, schematically depicted in figure (1) after Papazachos *et al.*, (2001), that has hosted the 365BC M = 8.3 event (Papazachos, 1990, Stiros, 2001, Shaw *et al.*, 2008), which is the largest known earthquake in the Aegean-Mediterranean convergence system.

Although several works have been published regarding the Miocene to Late Pliocene structural evolution of Crete based on the tectonostratigraphic column of the Neogene sediments and detail structural analyses (Kilias *et al.*, 1994, Fassoulas *et al.*, 1994, Jolivet *et al.*, 1996), information on the Late Pliocene to recent tectonic evolution and the corresponding fault activity (active or not faults) and their kinematics of Crete are much less available, with a limited number of publications on the Pliocene – Post-Pliocene brittle tectonics (e.g. Meulenkamp *et al.*, 1994, Duermeijer *et al.*, 1998, ten Veen & Meijer 1998, ten Veen & Kleinspehn 2003). The better understanding of the structural conditions under which this younger crustal deformation takes place is important for

Figure 1. Schematic geotectonic map of the broader Aegean area

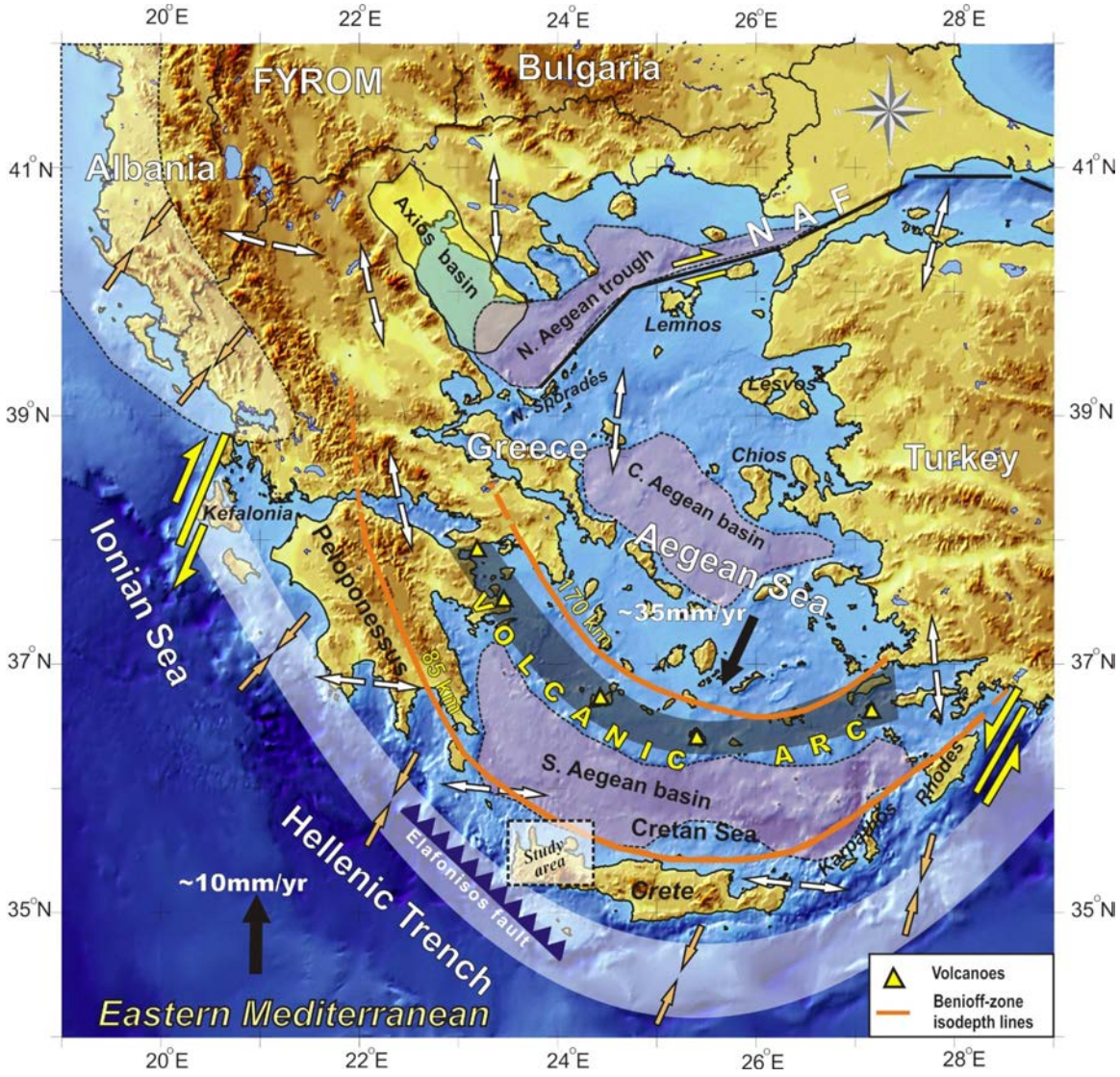

Plate motions in the southern Aegean area are depicted by solid vectors, while the local stress field is shown by double open arrows. The major Elafonisos thrust fault affecting the study area, as well as the main strike-slip zones (North Anatolia Fault-NAF, Kefallonia and Rhodes), the volcanic arc and the Benioff-zone isodepths are also presented (modified from Papazachos *et al.* 1998, Karagianni *et al.* , 2005).

theoretical, as well as for practical reasons (e.g. seismic risk mitigation policy in Crete), since these active structures are related to the medium-to-strong seismic activity on the island.

Our study focuses in the region of Western Crete (fig. 1). Within the framework of this study, the complicated fault system of Crete was mapped in detail and its kinematic and dynamic setting was analyzed, in order to distinguish the major active, possible active and geological (inactive) fault zones. The field study was completed by the analysis of fault-slip data recognized mainly along the main fault zones that dominate the study area. For the calculations we employed the slickenlines orientations and fault plane data (strike, dip direction and dip angle), as well as kinematic indicators (such as offsets, riedel fault, steps, folds, etc.) to determine the slip vector and the sense of movement (Hancock 1985). Furthermore, overprinting relationships based on the intersection of slip striae or displacements from earlier faults, as well as the stratigraphic age of the sediments that have been affected (or not) by the fault activity were used to distinguish fault generations of different age or different tectonic events.

Geological setting

The complicated nappes pile of the Crete Island have been stacked successively during the Alpine orogenic processes, from Jurassic to Miocene time (fig. 2), recording a multi-stage structural evolution. A major compressional regime has determined the evolution of the nappes stacking. Initially, the tectonic upper nappes (fig. 2, 3) were emplaced, successively followed by the other tectonic nappes from up towards down, with a SSW sense of movement. The whole tectonic nappes pile was finally emplaced on the lower nappes system, undergoing high pressure metamorphism during Upper Oligocene - Lower Miocene, through subsidence in a depth greater than 30km (fig. 2, 3, Seidel *et al.*, 1982).

Compression and nappe stacking were followed during Lower-Middle Miocene by a N-S collapse, tectonic thinning and extensional exhumation of the tectonic lower high-pressure nappes. These nappes emerged in a series of tectonic windows, while tectonic horsts and rather than subsidence subsequently evolved (Fassoulas *et al.*, 1994, Kilias *et al.*, 1994, 2002). The lower tectonic nappes were affected by ductile deformation, while the upper tectonic nappes by brittle low-angle extensional shear zones, respectively (Kilias *et al.*, 1994, Fassoulas *et al.*, 1994, Jolivet *et al.*, 1996). During this period, the first Neogene basins of the island were formed, often bordered by major syn-sedimentary normal boundary faults (fig. 4; Freudental 1969, Frydas & Keupp 1996). The main compression migrated southwards towards the Mediterranean ridge, where the present active subduction zone of the Eastern Mediterranean lithosphere beneath the Aegean microplate is currently taking place.

The extensional tectonic regime after Middle Miocene is characterized by an initial almost N-S sub-horizontal extension and simultaneous thinning of the crust. Younger neotectonic faults followed this tectonic process in Crete, due to the ongoing active Southern Aegean subduction.

Figure 2. Geological map indicating the tectonic lower and upper nappes of the Crete nappes pile

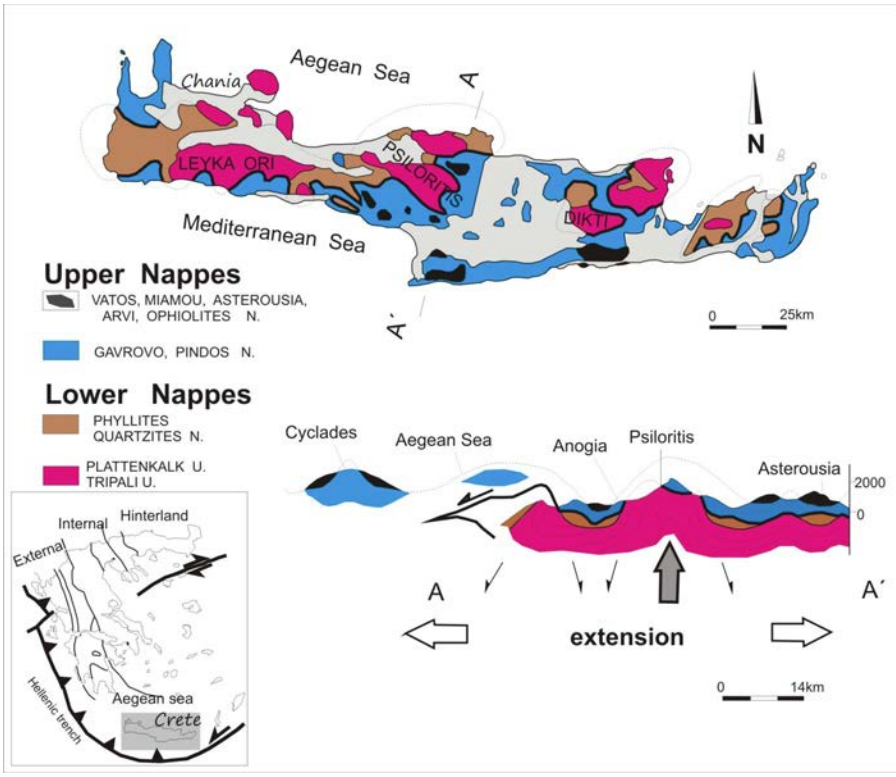

(modified from Kilias *et al.* 1994).

Figure 3. The complicated tectonic nappes pile of Crete

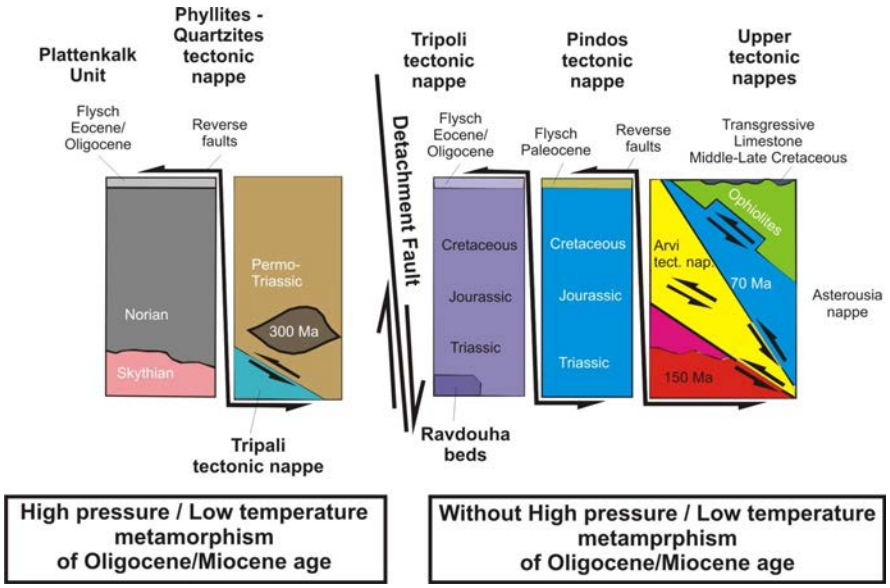

(modified from Seidel *et al.* 1982).

Figure 4. Lithostratigraphic column of the Neogene in Western Crete

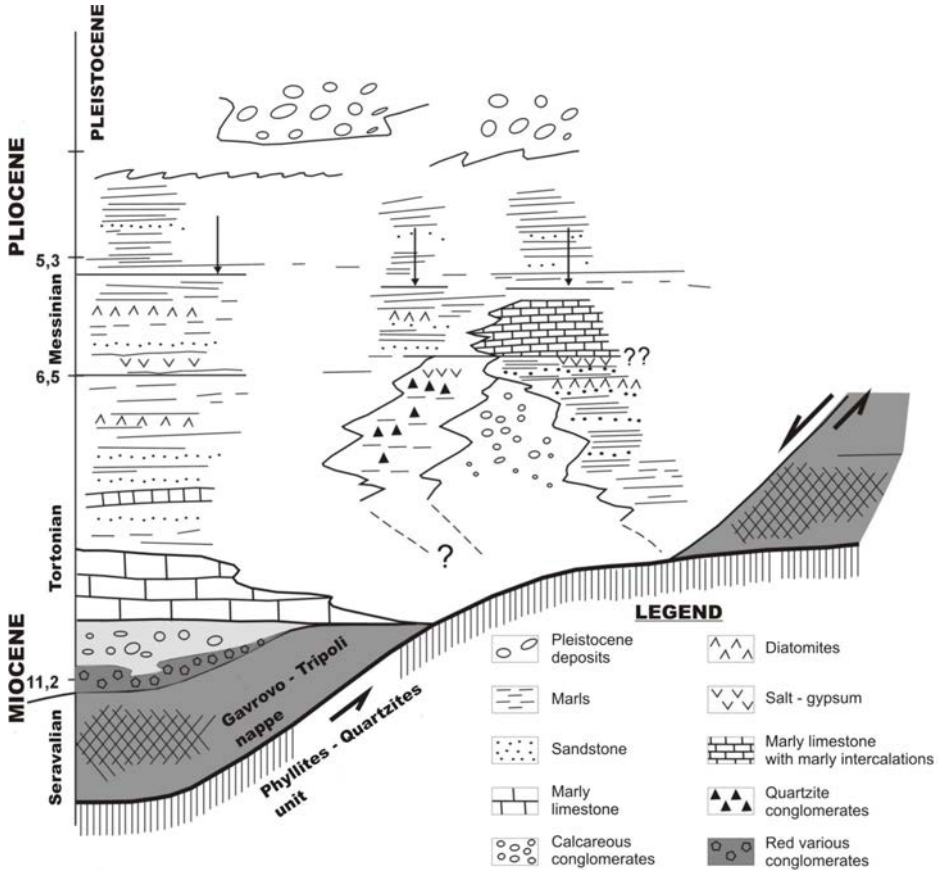

(modified from Freudental 1969 and Frydas & Keupp 1996).

Brittle neotectonic analysis - Active stress field

The detailed study of the brittle neotectonic deformation in Western Crete, suggests the presence of two main brittle Neogene tectonic events (D_1 & D_2), generating the fault network of Western Crete (fig. 5 & 6). The first D_1 tectonic event took place from Middle/Upper Miocene to Upper Pliocene, as it affects the basins' sediments of Miocene and Pliocene age, but not the younger Quaternary deposits.

The major normal faults in Western Crete of E-W strike, which in some cases locally deviate to ENE-WSW and ESE-WNW, have been formed during this D_1 event. These faults dip mainly to the north at high angle and they usually correspond to the initial boundary fault zones of the Neogene basins of Western Crete. Essentially, they represent the stage immediately following the initial Miocene expansion collapse of the Crete nappes pile along low angle normal detachment faults, with both events showing the same dynamics and kinematics.

Figure 5. Neotectonic - geological map of Western Crete

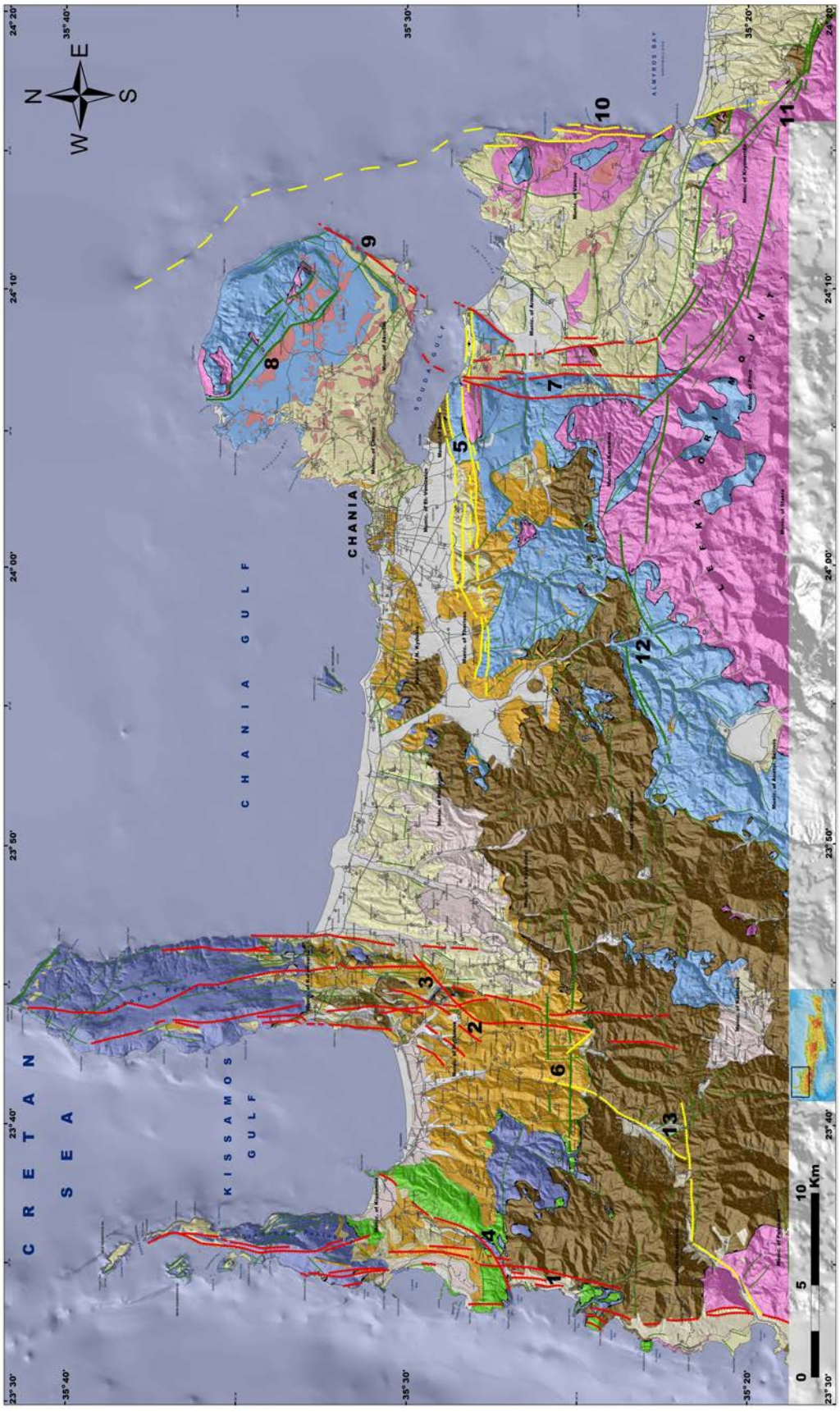

Figure 6. Seismotectonic map of faults and surface earthquakes' epicenters of Western Crete.

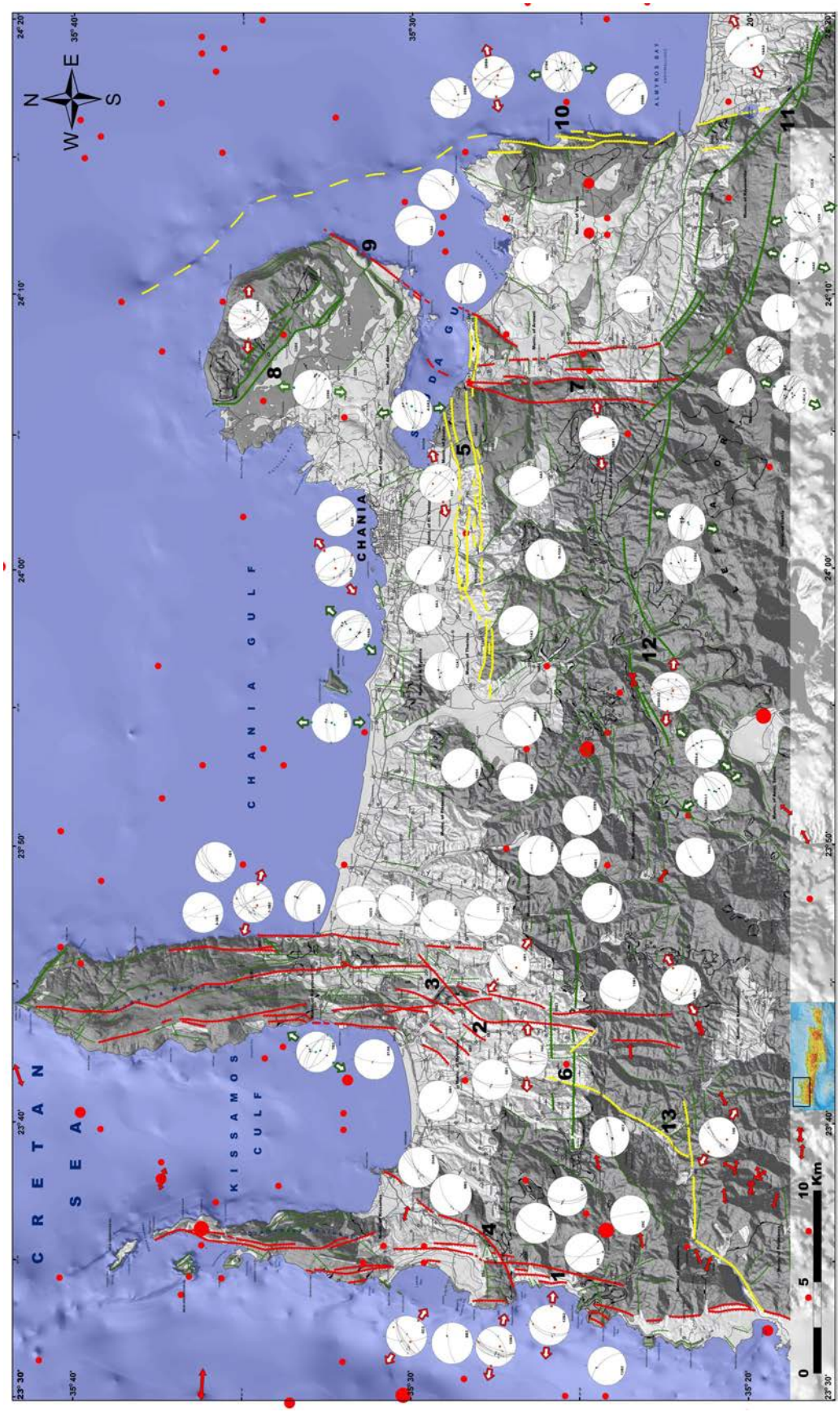

Figure 5a. Map legend for Figure 5

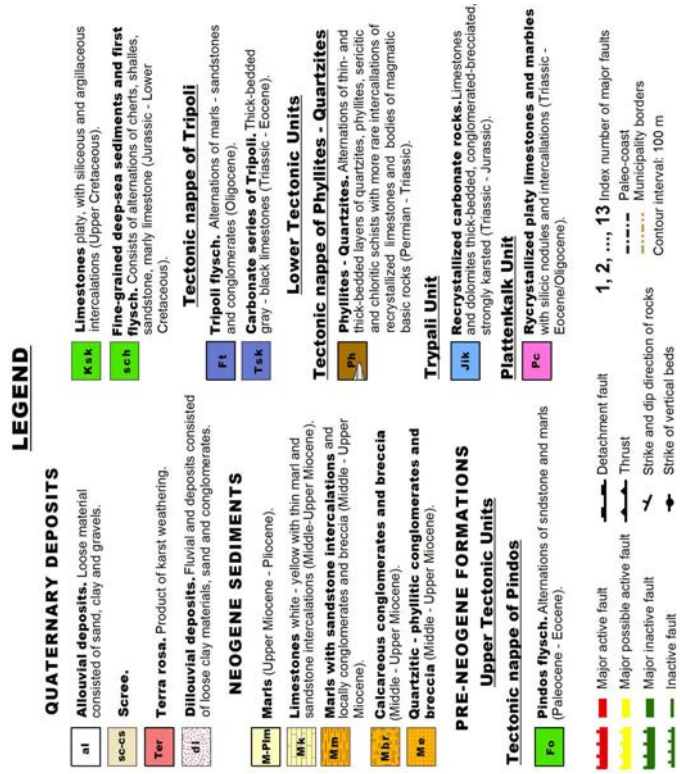

Figure 6a. Map legend for Figure 6

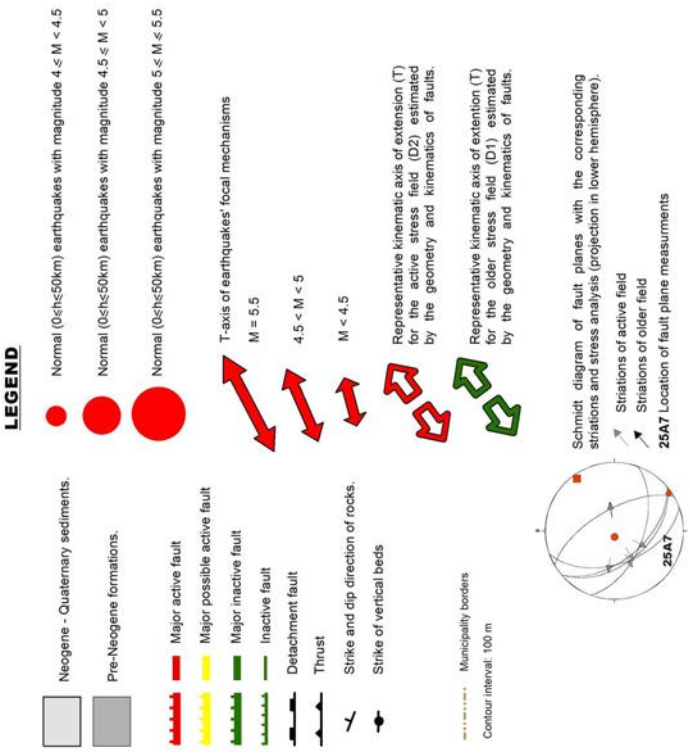

Figure 7. Photos showing influence of the faults to Pliocene and Pleistocene sediments

a. Influence of Malaxa – Souda's Gulf fault to Pleistocene sediments. b: Topolia fault displaying strike-slip movement, showing offset structures.

Figure 8. Representative paleostress diagrams of $\sigma 1 > \sigma 2 > \sigma 3$ for the older D_1 tectonic event

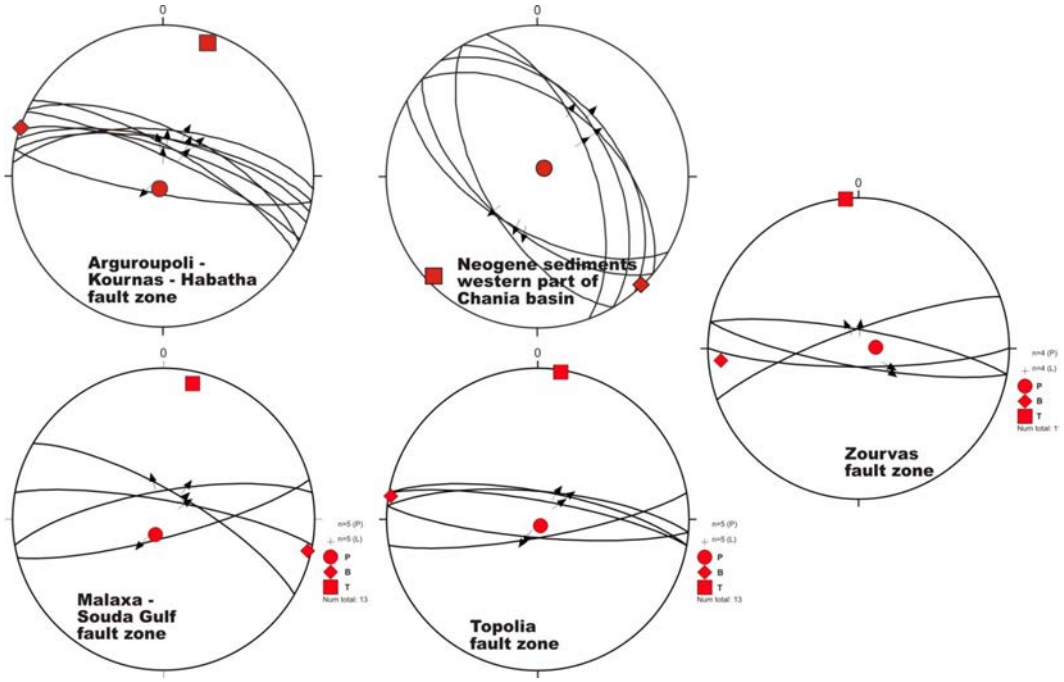

(lower hemisphere projection) by P-T method (Turner 1953) (see text for explanation).

Figure 9. Representative paleostress diagrams of **σ1>σ2>σ3** for the younger D_2 tectonic event

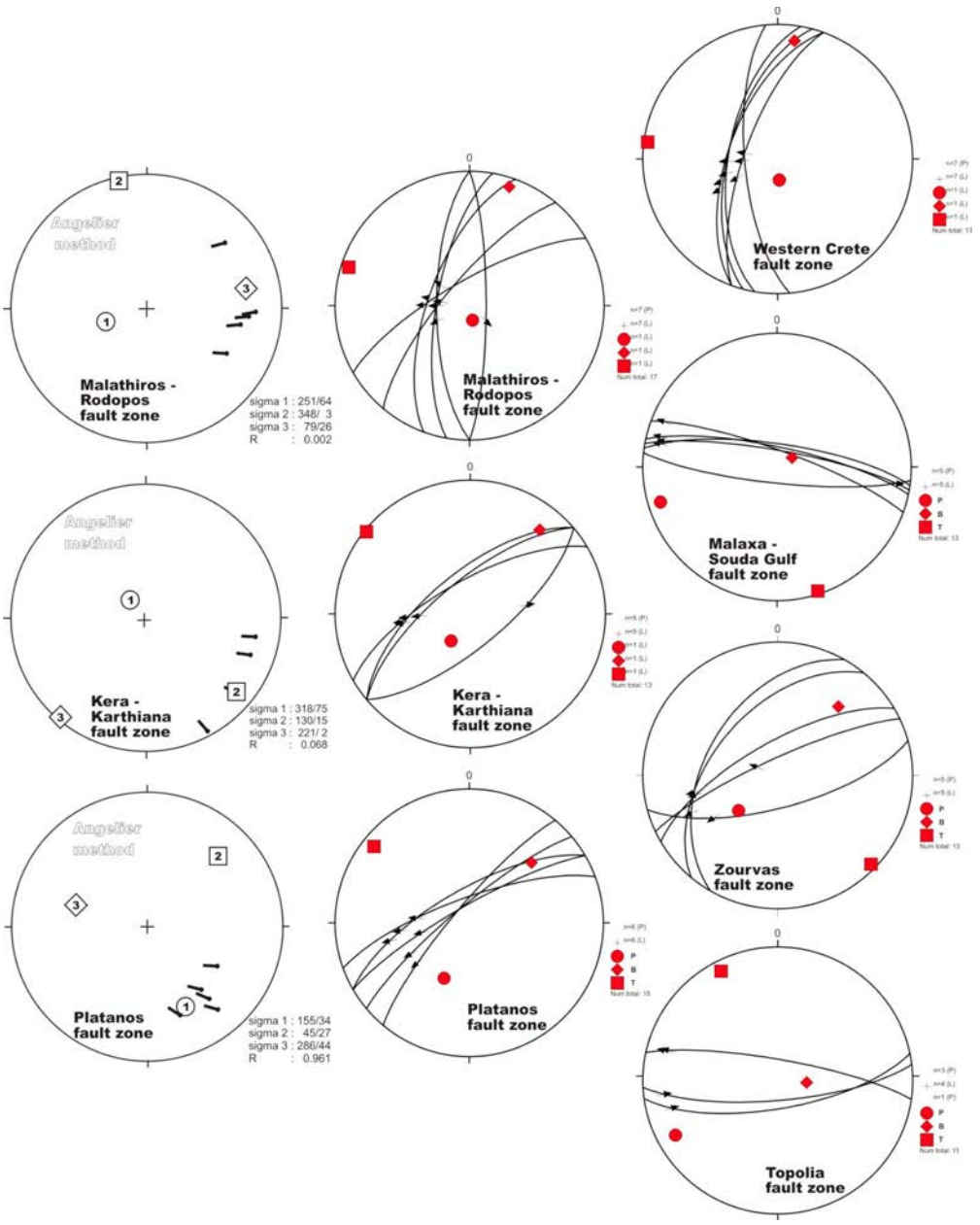

(lower hemisphere projection) by Angelier 1979 and Angelier *et al.* 1982 inverse method and P-T method (Turner 1953) (see text for explanation).

The kinematic analysis of the D_1 faults shows that they are normal faults with mostly normal dip-slip component. This is verified by the presence of high angle striations identified on the fault planes, dipping mostly towards the NNE to NNW. The NNW slip motion corresponds to the relatively younger slip motion associated with the D_1 phase. Moreover, minor oblique normal faults trending NW-SE and NE-SW are also related to the D_1 kinematics, showing significant sinistral or dextral horizontal component of motion, respectively. Paleostress analysis for the D_1 event, using the inverse method of Angelier 1979, Angelier *et al.*, 1982 and P-T method (Turner 1953), shows a low dipping angle minimum σ3-stress axis with a strike varying between NNE-SSW to NNW-SSE (fig. 8 & 9) for both methodes. The program Stereonett (Duyster 2000) has been used for graphical presentation of the structural data.

The second D_2 tectonic event took place from Upper Pliocene up to present. Faults of this event overprint the previous D_1 faults, affecting usually the cataclastic fabric along the D_1 fault zones. Moreover, the D_2 faults clearly affect the Pliocene sediments and have also been detected in recent Quaternary deposits (fig. 7). Faults related to the D_2-event are mostly major faults of N-S strike, varying from NNW-SSE to NNE-SSW, with a dip direction mostly towards West. These normal faults exhibit a significant downwards dip-slip component of motion and striations dipping on the fault surfaces towards North or South in a high angle pitch (almost 75-85°). Moreover, faults of mainly NE-SW strike (occasionally also of NW-SE strike) are also closely related to the D_2 kinematics. These are oblique-normal faults with significant sinistral or dextral horizontal component of motion. Some of these faults (mainly those of NE-SW strike) seem to form major transitional rupture zones between segments of the dominant N-S faults. However, older D_1 striations are recognized on the fault surfaces of these D_2 phase oblique-normal faults, revealing a possible reactivation during D_2 tectonics, though they were initially created during the D_1 event. The D_2 kinematics are also often imprinted on the older E-W traced D_1-faults by their reactivation as sinistral strike-slip faults. This pattern can be derived from the observation of horizontal striations on the fault surface, almost perpendicular to the older ca. dip-slip D_1-striations.

Paleostress analysis for the D_2 tectonic event using the methods of Angelier 1979, Angelier *et al.*, 1982 and P-T method (Turner 1953) shows a sub-horizontal minimum $\sigma 3$-stress axis, with strike ranging from WSW-ENE to WNW-ESE, with the second stress direction being the younger one. This pattern is in excellent agreement with the active stress field along a narrow zone lying between the external NW-SW compression (due to the Eastern Mediterranean subduction under the Aegean) and the inner, back-arc ~N-S extension (e.g. Papazachos *et al.*, 1992, Papazachos and Kiratzi, 1996). This narrow zone extends all the way from the Albania-Greece border and the main body of the Hellenides mountain chain up to Peloponnesus, Crete and Rhodes, following the shape of the Hellenic arc. However, its exact spatial extent is not clearly defined, since it locally exhibits partial overlapping, especially with the N-S extension area, e.g. in western Macedonia and Epirus, (Mountrakis *et al.*, 2006).

In order to explore the specific characteristics of the latest D_2 phase observed in active faults and its spatial relation with the active stress field, we employed the available fault plane solution data for the study area. Our approach was realized in two steps. In the first step, all available fault plane solutions published for the broader study area were collected. The main data sources were Harvard, INGV and ETH, which publish solutions on a relatively regular basis for a large number of earthquakes (typically $M > 4.5$). Moreover fault plane solutions from a large number of publications (e.g. Lyon Caen 1988; Liotier 1989; Louvari, 2000) were also collected. In general, 3 main types of faults are recognized from the corresponding spatial distribution:

a) Thrust-type fault plane solutions (fig. 10a), with a dominant NW-SE direction, following the general local trend of the Hellenic arc. The corresponding earthquakes occur mostly in the Ionian Sea and the Mediterranean area, south of the coasts of Crete (e.g Elafonisos fault area-fig. 1), Kythira and Peloponnesus, with depths mainly in the range of 20-50km

Figure 10. Regional focal mechanisms in the broader SW Aegean area compiled from several published sources

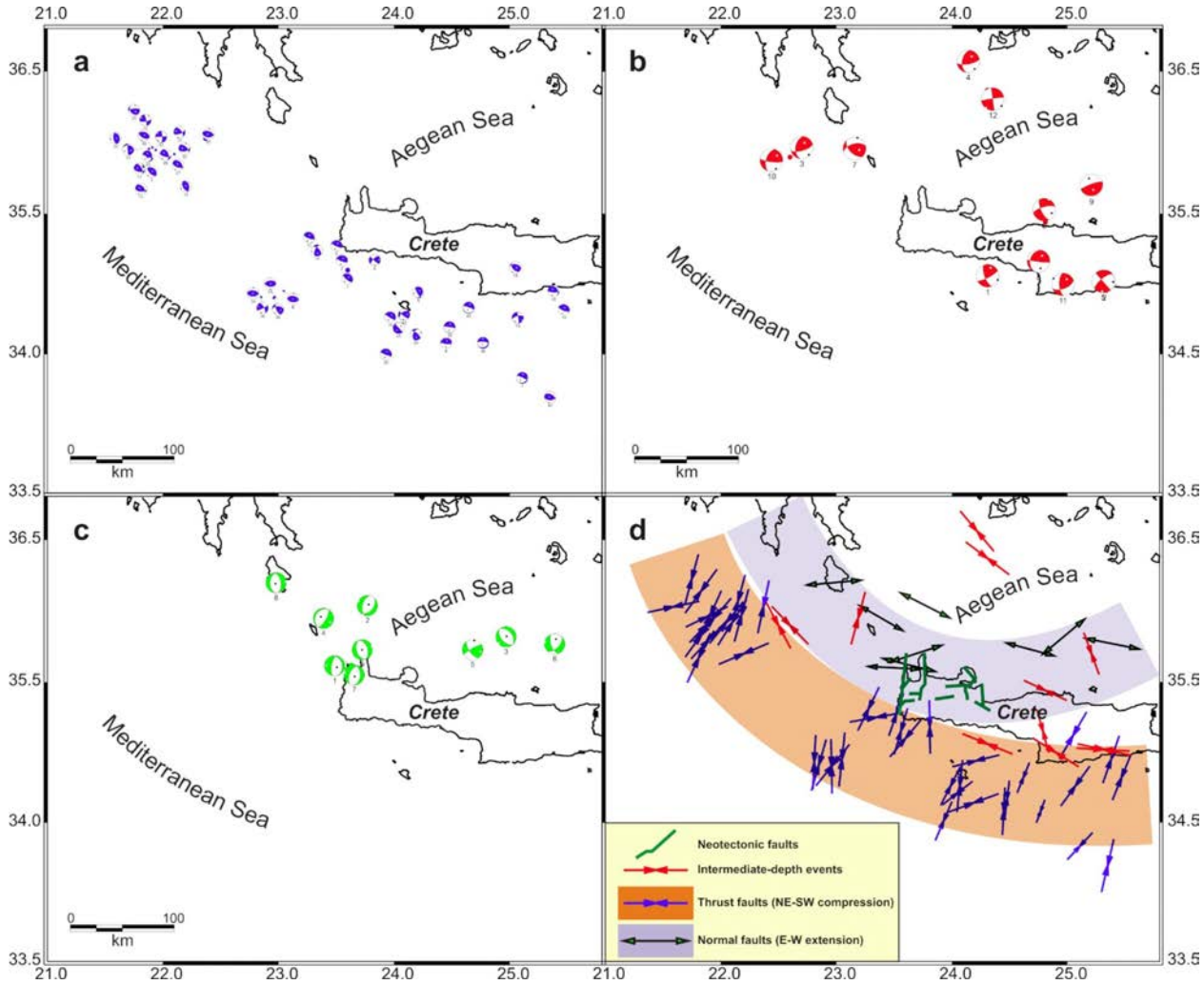

a) Thrust-type events along the outer Hellenic-arc (blue arrows), b) Intermediate-depth strike-slip events (depths 50-120km) with significant thrust component (orange arrows), c) Normal-type events (black-green arrows), showing a dominant roughly N-S strike. d) Spatial distribution of the corresponding sub-horizontal (dip <30°) principal axes in the study area, showing the clear separation of the NW-SW compression area in the outer arc with the E-W extension area along the Kythira-NW Crete area. Intermediate-depth events exhibit a typical inslab-parallel compression. The 13 main faults mapped in this study are schematically depicted with green lines.

b) Strike-slip events with a significant thrust component (fig. 10b), corresponding to intermediate-depth events along the subducted Benioff zone, at depths gradually increasing from 50km (in the Crete-Kythira area) to ~100-120km in the southern Aegean volcanic arc region (fig. 1).

c) Normal-type events, with a roughly N-S direction (fig. 10c), which occur at shallow depths in the Kythira and NW Crete area, extending in the Cretan basin, just north of the Crete mainland.

Though, the determined fault plane solutions show local variability, the corresponding distribution of the sub-horizontal (dip <30°) principal stress axes shows a more consistent setting, presented in figure (10d). The distribution presented in this figure shows a clear separation of the outer-arc NE-SW compression from the E-W extension regime in the Kythira and NW Crete mainland. The last one is in very good agreement with the stress field of the previously presented D_2 phase. In the same figure the traces of the 13 main faults identified in the present study (later presented in detail) are also schematically depicted.

In order to further examine this issue, we have also collected additional fault plane solutions determined from local temporary networks installed in western Crete or the broader area (Besnard, 1991; Chabalier *et al.*, 1992; Hatzfeld *et al.*, 1993; Jost *et al.*, 2002). The corresponding distribution (also solutions from the regional database of figure 10 for the study area) is presented in fig. (11a), including mainly small events with M in the range -0.2 to 3.8. Although, in a few cases alternative solutions are presented, the corresponding principal sub-horizontal (dip < 30°) extension axes distribution is quite consistent (fig. 11b), showing a dominant E-W extension. Using the resulting distribution, an average σ3 extension axis was determined using the stress-tensor inversion method of Gephart and Forsyth (1984) and the average moment-tensor method of Papazachos and Kiratzi (1992). These results, also presented in fig. (11b) with large arrows, verify: a) The presence of an active E-W to WNW-ESE extension in western Crete (compatible with the D_2 phase recognized from active faulting) and, b) the spatial extent of the extension regime, which covers the whole western Crete mainland, showing that the E-W extension controls the upper crustal deformation pattern throughout the whole study area, as also depicted in fig. 10d.

Figure 11. Fault plane solutions and stress-axes from microseismicity in Western Crete

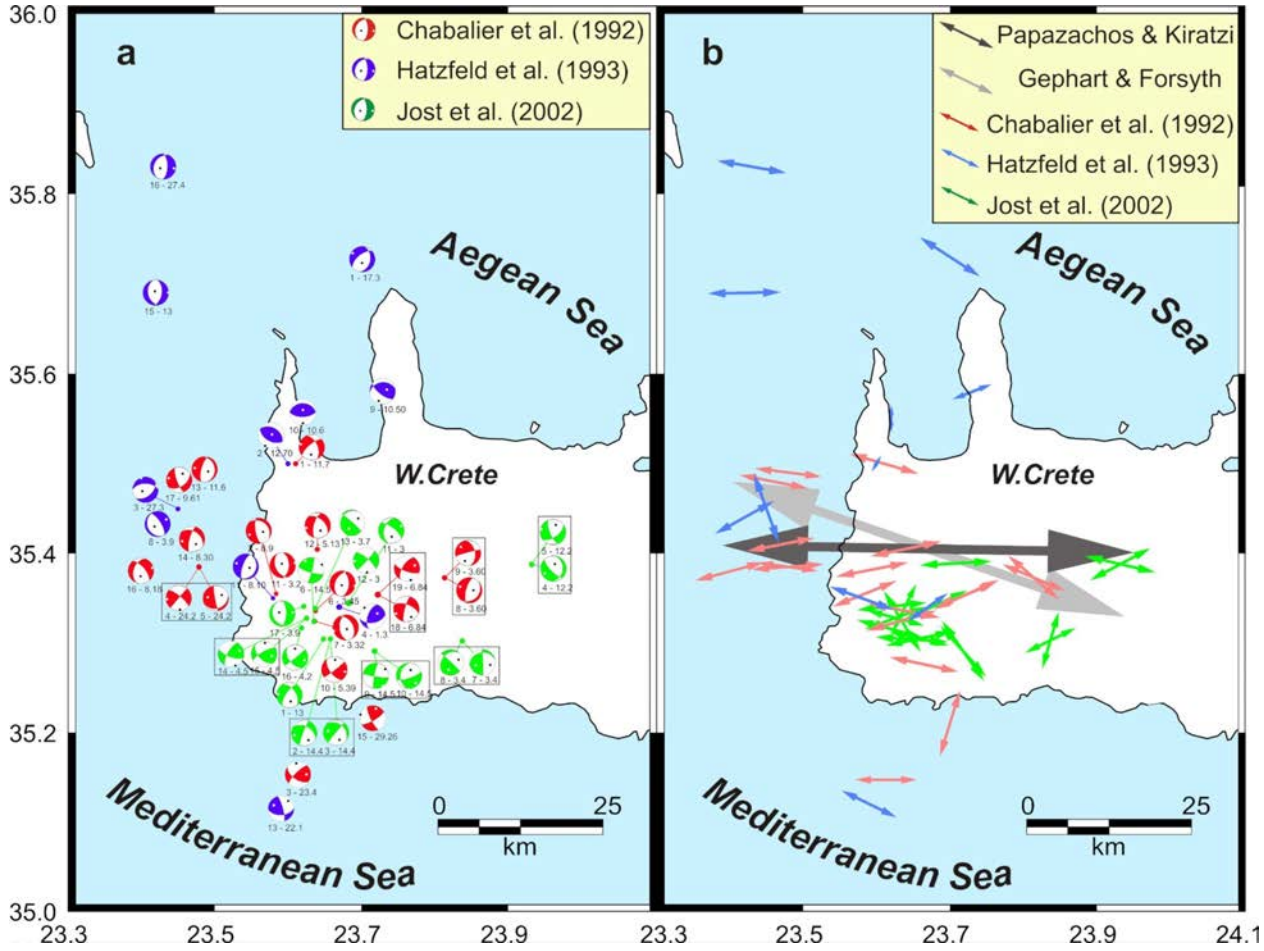

a) Fault plane solutions for small-magnitude events in Western Crete. b) Spatial distribution of the corresponding sub-horizontal (dip <30°) principal extension axes. The average stress, computed with the methods of Gephart and Forsyth (1984) and Papazachos and Kiratzi (1992), are also presented with large grey and black arrows respectively.

Record of the major neotectonic faults of Western Crete

Several of the faults, activated during the D_2 phase, display clear indications of recent activity, on the basis commonly accepted geological criteria (Hancock 1985, Suppe 1985), hence they were considered as geologically active or possible active faults. From the complicated D_1 and D_2 fault systems in Western Crete described previously, 13 major normal faults of high dip-angle were identified, which exhibit clear activation from Middle-Upper Miocene till today. These faults are numbered 1 to 13 in the neotectonic-geological and seismotectonic maps (e.g. fig. 5, 6) and are analyzed in detail in the following:

1. The Fault of Western Crete (fig. 12) is a rupture zone of significant length (> 40km) and a N-S strike, dipping to the West and directly related to D_2 tectonics. The fault shapes the western coast of Crete and it is composed of several segments, the most important of which are the Gramvousa (11 km), Falasarna - Sfinari (11 km) and Kampos - Stomion (10 km) segments. These segments cut the basement rocks (the HP/LT phyllite - quartzite unit and limestones of Tripolis and Pindos zones), as well as the Neogene sediments. Moreover, their recent activity affects their own tectonic scree found in older terraces, as well as the erosion materials in more recent terraces.

Figure 12. Neotectonic-geological map and geological cross-section of the Western Crete fault zone

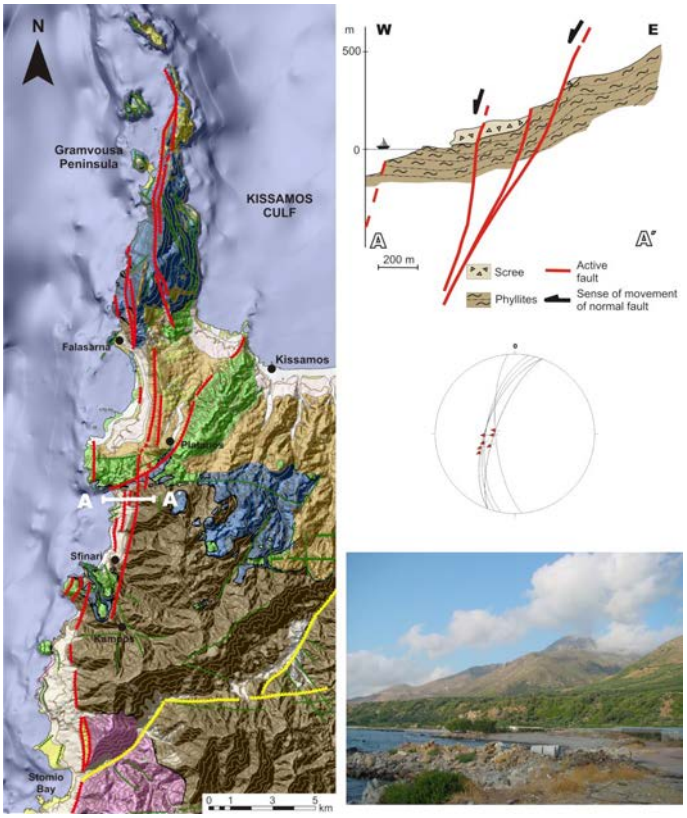

(for map legend see fig. 5). Schmidt diagram (lower hemisphere projection) showing the kinematics of the fault zone, compatible to D_2 event. Photo: Western Crete fault affecting tectonic scree of terraces.

All segments are characterized as active faults using geological criteria, such as the influence on recent aeolian sand assemblages in the coastal area, the vertical and curved slopes of streams, the cutting of the recent tectonic scree etc. The present rupture of the fault zone in the terrestrial area represents the initial trace of the fault, thus corresponding to its initial activation. Following this initiation, the tectonic activity was transferred in the sea, hence the active fault zone is located in the sea area, westwards of the present coast line. This is supported be series of historic earthquake epicenters reported by Armijo *et al.*, (1992) for the submarine area in the western coast, with T-axis of E-W strike, a fact that supports the employed geological criteria for its characterization as an active fault. It should be noted that Beneke *et al.*, (2002) have calculated a 0.75 to 1.5 mm/yr uplift rate of the land during Quaternary, due to the tectonic activity of the Western Crete fault zone (fig. 12) .

2. The Fault of Malathiros - Rodopos (fig. 13) is also a large (30km) fault zone related to D_2 tectonics, trending N-S and also dipping westwards. It's composed by three main segments, namely the Rodopos (18 km), Kera (4 km) and Malathira (9 km) segments. Several additional fault branches, parallel to the main fault zone, are also identified in the field, as well as antithetic conjugate faults dipping eastwards. The segment of Kera is curved towards the NE and represents a rather dextral transfer fault between the other two segments. Along all segments, especially this of Kera, epicenters of mainly historic surface earthquakes are recorded.

Figure 13. Neotectonic-geological map and geological cross-section of the Malathiros-Rodopos fault zone

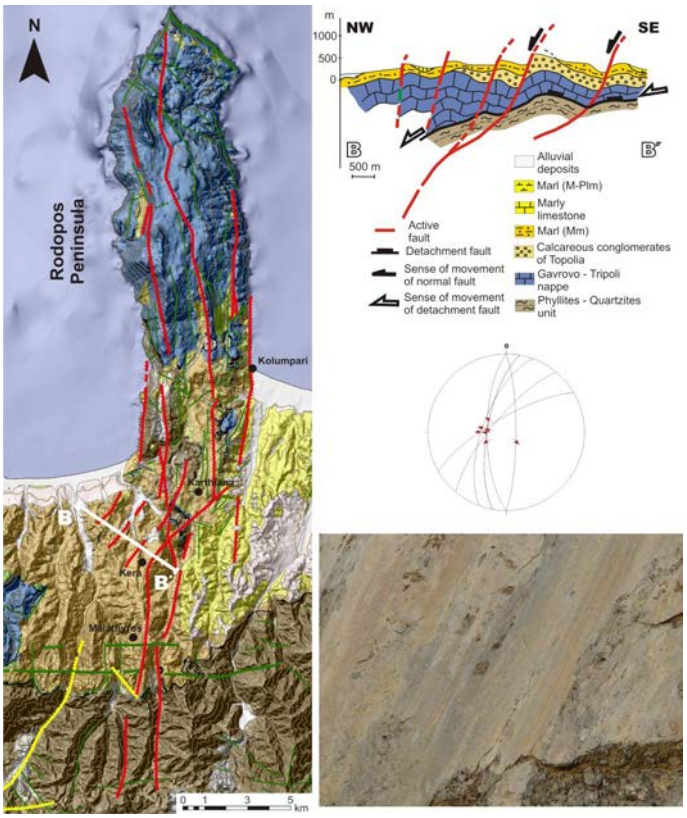

(for map legend see fig. 5). Schmidt diagram (lower hemisphere projection) showing the kinematics of the fault zone, compatible to D_2 event. Photo: fault plane with striations.

The fault zone cuts many of the Alpine basement rocks, as well as Miocene-Pliocene marl sediments, causing a sharp change of their dipping angle, resulting even in a vertical pattern of their bedding (e.g. in the area of the Malathira village). In some cases, the activity of this fault's segments is recognized in Pleistocene and younger scree of their rupture surfaces. For these reasons, all segments are considered as active faults with successive tectonic activity regarding the evolution of the fault zone.

Figure 14. Neotectonic-geological map and geological cross-section of the Kera-Karthiana fault zone

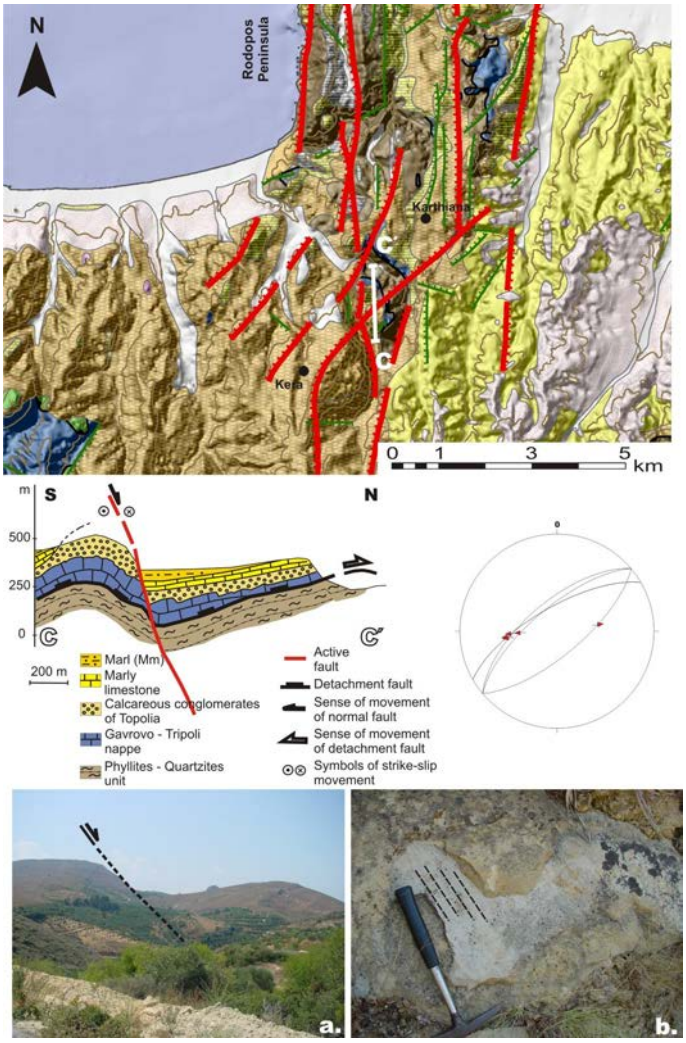

(for map legend see fig. 5). Schmidt diagram (lower hemisphere projection) showing the kinematics of the fault zone, compatible to D_2 event. Photo: a. A panoramic view of the fault zone, b. Fault plane with striations.

3. The Fault of Kera - Karthiana (fig. 14) was previously described as a transfer active fault between the segments of Malathira - Rodopos fault zone. It has a NE-SW orientation, with a high dipping angle towards the NW and an average length of 4 km, causing an impressive downthrow and tilting of the Neogene sediments. Though it is closely related to the N-S fault of Malathira - Rodopos, it is considered to have a later occurrence or

activation, since it influences recent red Pleistocene and scree sediments (fig. 14, 16).

4. The Fault of Platanos (fig. 15) exhibits a NE-SW strike and dips towards the NW. The fault is characterized by an important sinistral horizontal component of motion, related to the D_2 tectonics. It clearly overprints the N-S oriented Western Crete fault, thus the Fault of Platanos can be characterized as a lateral-normal active fault (fig. 16).

Figure 15. Neotectonic-geological map and geological cross-section of the Platanos fault zone

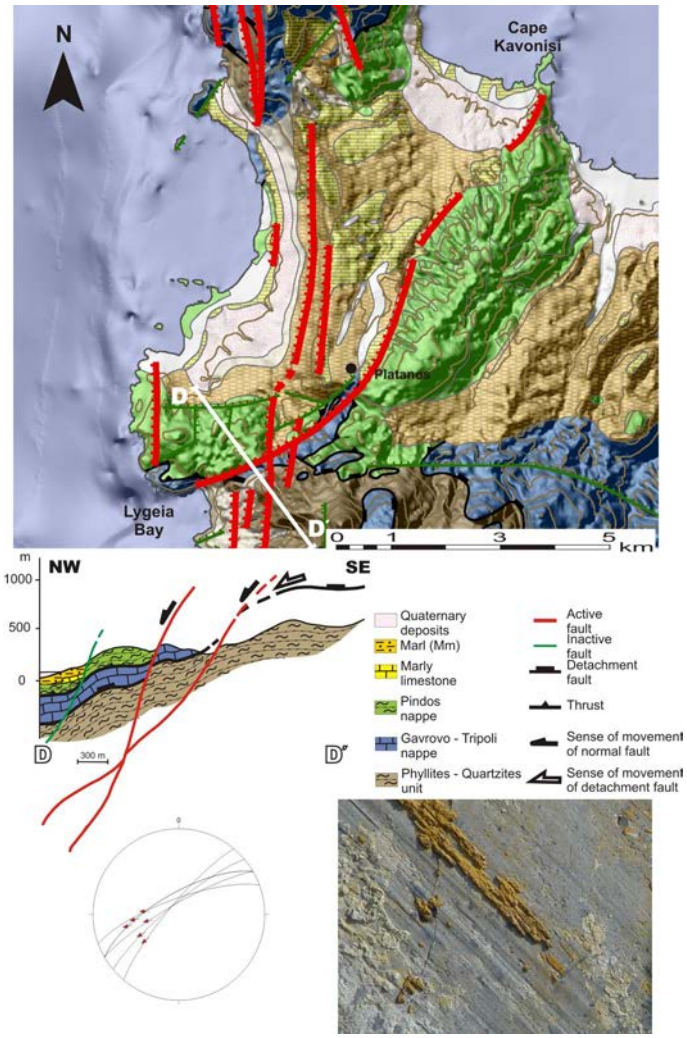

(for map legend see fig. 5). Schmidt diagram (lower hemisphere projection) showing the kinematics of the fault zone, compatible to D_2 event. Photo: striation on the fault plane with important sinistral strike-slip component.

Figure 16. Photos showing influence of the active faults to Quaternary and recent sediments, as well as interaction between the faults

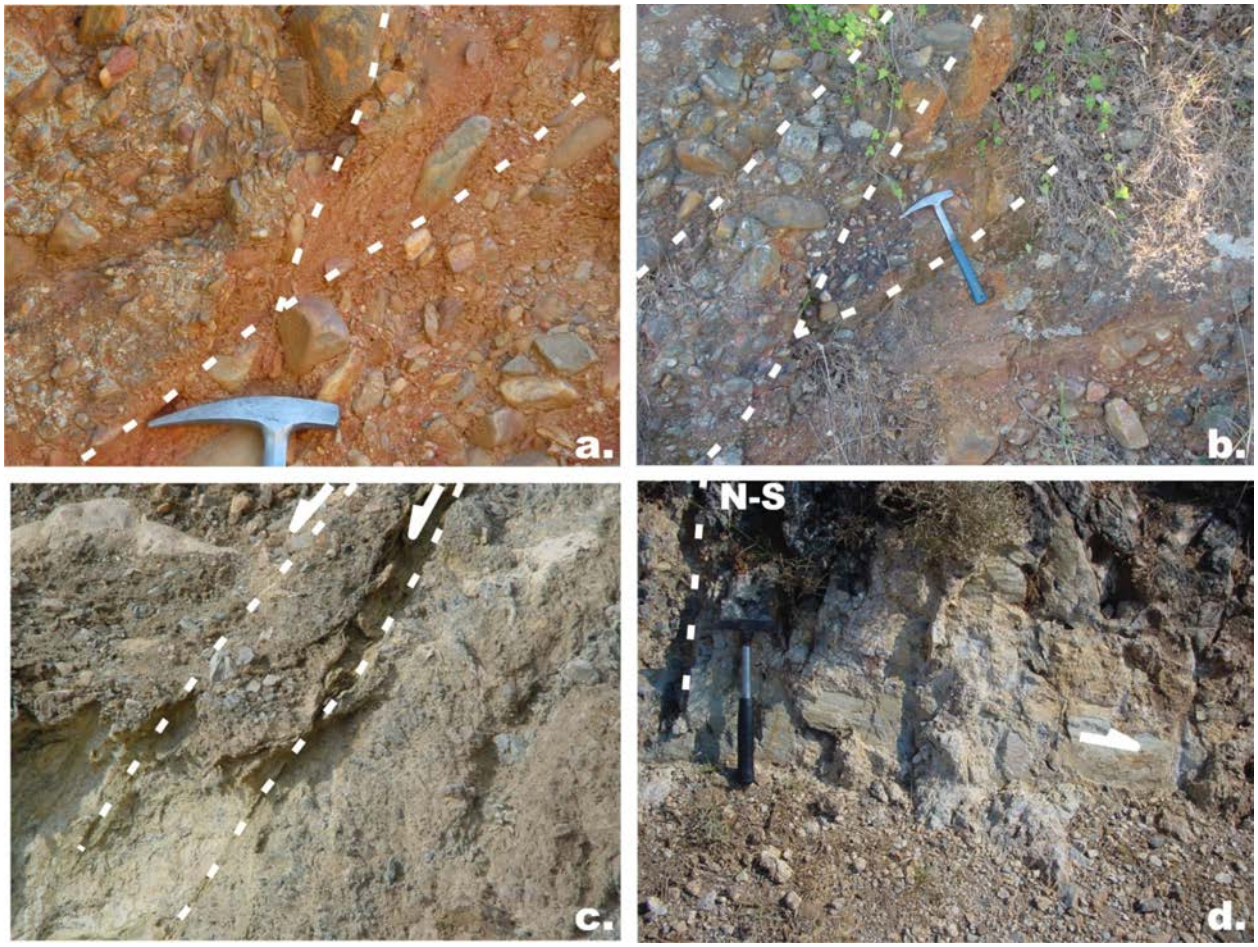

a, b: Influence of Kera - Karthiana fault to Quaternary deposits. c: Influence of Western Crete fault to recent erosion materials. d: Interaction between both active fault zones, those of Platanos (with an important strike-slip component) and Western Crete.

5. The Malaxa - Souda's Gulf Fault (fig. 17) corresponds to a high length (> 20km) fault zone of E-W strike, dipping towards the North and forming the tectonic graben of Myloniana - Mournies - Souda's Gulf. The fault zone is composed by a series of parallel fault surfaces, which were formed due to successive fault activity and migration towards the North. Thus, successive tectonic terraces were created, with impressive cataclastite on the Mesozoic Trypali limestone and corresponding gradual subsidence of the tectonic graben. The northernmost and relatively younger branch separates Neogene marls from Pleistocene sediments and causes impressive vertical bedding of the first ones.

Figure 17. Neotectonic-geological map and geological cross-section of the Malaxa - Souda's Gulf fault zone

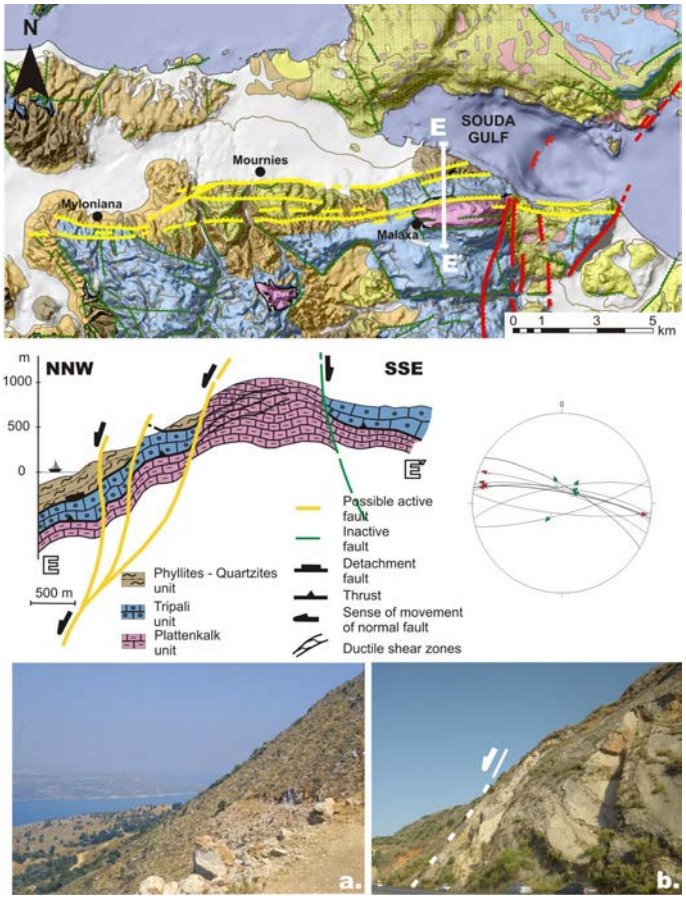

(for map legend see fig. 5). Schmidt diagram (lower hemisphere projection) showing the kinematics of the zone, compatible to both D_1 (green) and D_2 (red) event. Photo: a. The fault zone creating the sharp slope of Souda's graben, b. Vertical bedding of Miocene - Pliocene marls of Souda's graben caused by the fault's activity.

Two main slip patterns were observed on the fault surfaces: The first (older) one is related to an important dip-slip component of motion, clearly linked to the D_1 extensional event of Upper Miocene - Lower Pliocene age, when the sharp relief of the Souda's trough was formed. The second (younger) event is related to a mainly sinistral horizontal component of slip (accompanied by a minor dip-slip component) related to the D_2 event and acting from Upper Pliocene-Quaternary up to today. In this sense, the fault zone is considered as possibly active, though its orientation isn't compatible to the previously described active stress field.

6. The Topolia Fault (fig. 18) represents a fault zone of 10 km length, E-W strike, dipping northwards, related to the D_1 extensional event. The Topolia fault evolved as a synsedimentary fault zone related to the initial opening of the Neogene basin of the area during Tortonian. However, on its fault surfaces, younger striations are observed, representing a pure strike-slip motion, compatible to the D_2 kinematics. These observations suggest that the fault zone has been reactivated as a strike-slip one during more recent times (Upper Pliocene – Quaternary), showing a similar to the Malaxa - Souda fault evolution.

Figure 18. Neotectonic-geological map and geological cross-section of the Topolia fault zone

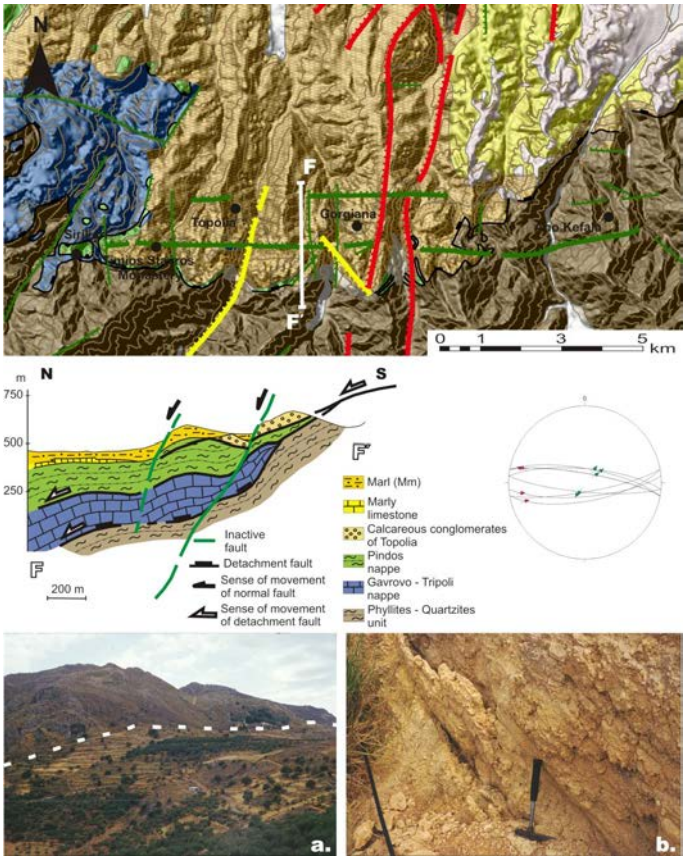

(for map legend see fig. 5). Schmidt diagram (lower hemisphere projection) showing the kinematics of the fault zone, compatible to both D_1 (green) and D_2 (red) event. Photo: a. Panoramic view of the fault, b. Offset structures along the fault, related to the D_2 activity.

7. The Zacharias - Pemonia Fault (fig. 19) is a large fault zone in the western part of the Neogene basin of Apokoron. This fault has a N-S strike and a gradual step-like fall towards the East through a system of parallel fault branches, involving a total length of 11km. This fault system affects the Neogene sediments and forms the Apokoron basin by successive tectonic terraces,

impressive slickensides, cataclastic phenomena and surface openings. Its kinematics are compatible to the active stress field, hence it is characterized as an active fault zone.

Figure 19. Neotectonic-geological map and geological cross-section of the Zacharias - Pemonia fault zone

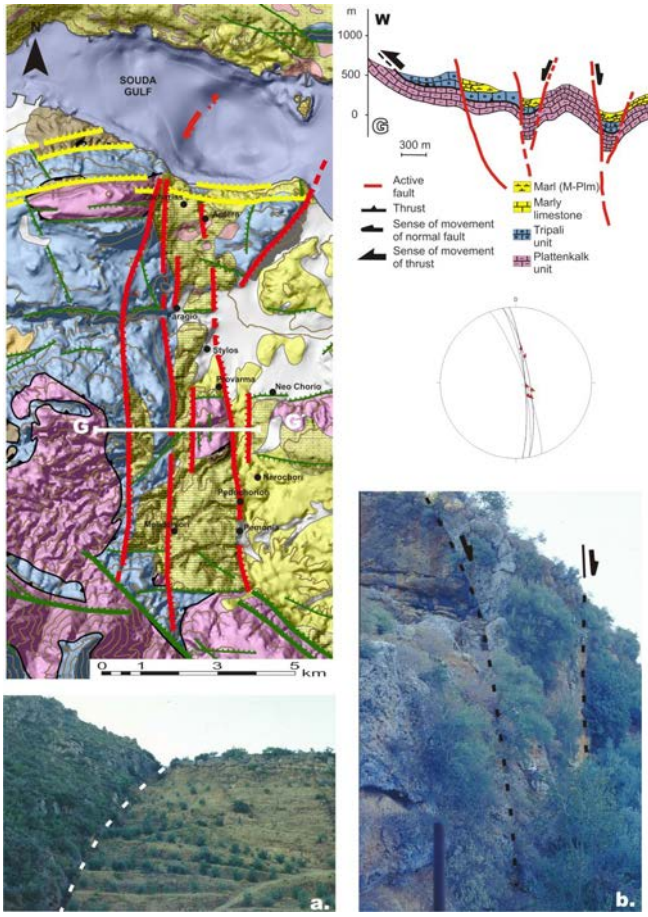

(for map legend see fig. 5). Schmidt diagram (lower hemisphere projection) showing the kinematics of the fault zone, compatible to D_2 event. Photo: a. A segment of Zacharias - Pemonia active fault zone displaying surface opening, b. Cataclastic zone along Zacharias - Pemonia fault.

8. The Akrotiri Fault (fig. 20) develops in a NW-SE strike, dipping in a high-angle towards the SW. It is composed by parallel faults in a characteristic "doublex" structure, forming tectonic terraces and the large plateau of Akrotiri, with a total observable length of 11km. Although its orientation is not compatible to the active stress field, the kinematics and geometry of the fault indicate that it was activated during D_2 event, as on its fault plane an oblique downwards sense of slip is recognized by the observed striations and other kinematic indicators.

Figure 20. Neotectonic-geological map and geological cross-section of the Akrotiri fault zone

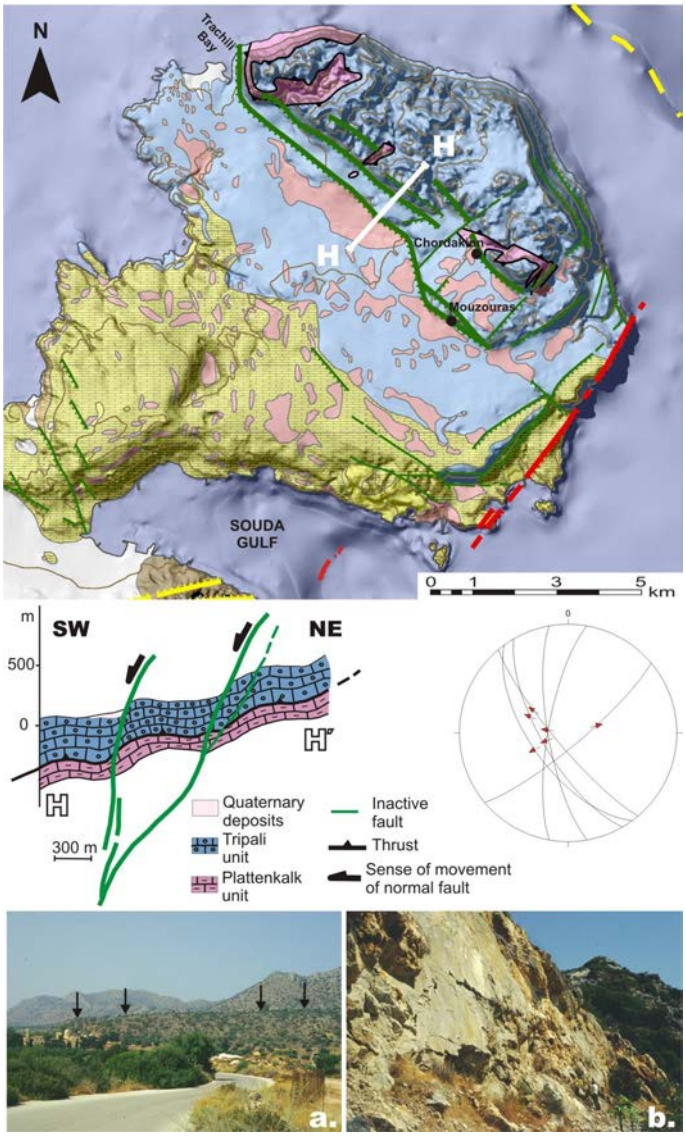

(for map legend see fig. 5). Schmidt diagram (lower hemisphere projection) showing the kinematics of the fault zone, compatible to D_2 event. Photo: a. Tectonic terrace created by the fault activity, b. Fault plane of Akrotiri fault with oblique striations.

9. The Fault of Marathi (fig. 21) develops along the SE edge of the Akrotiri Peninsula, forming its high-angle dipping slopes. The fault trends NE-SW, dipping in a high angle towards the SE. Its continuation beyond Souda's Gulf is also recognized in the Ancient Aptera archaeological site. Apart of the basement rocks, the fault intersects the last Pleistocene terrace of Akrotiri fault, showing that the Marathi fault is clearly younger. The kinematics and geometry of the fault are compatible to

the D_2 event and it is considered to have a recent Quaternary activity.

Figure 21. Neotectonic-geological map and geological cross-section of the Marathi fault zone

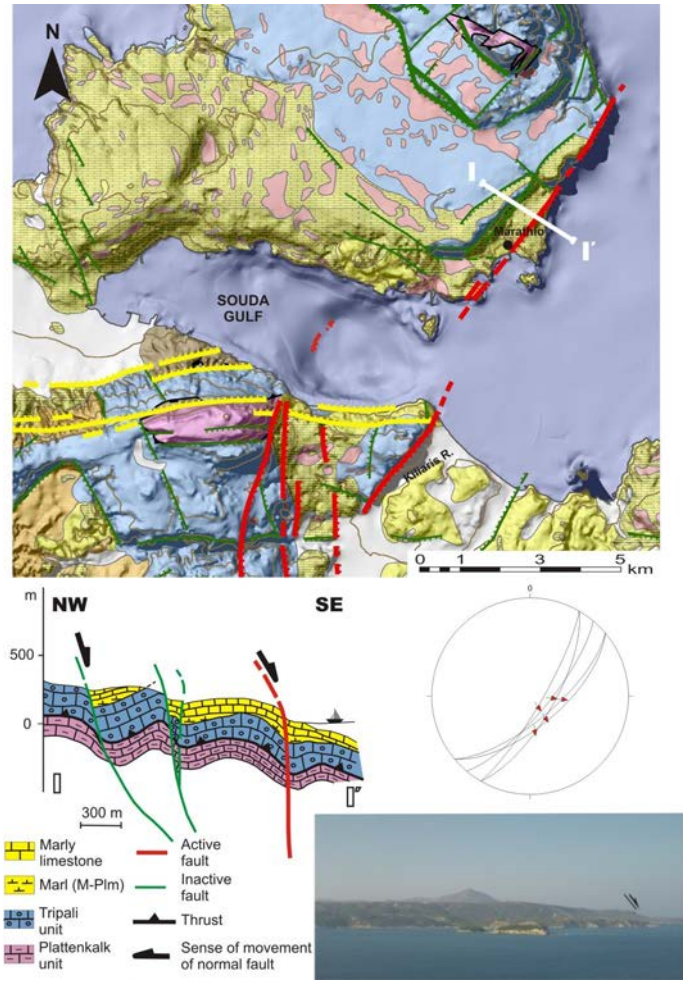

(for map legend see fig. 5). Schmidt diagram (lower hemisphere projection) showing the kinematics of the fault zone, compatible to D_2 event. Photo: a panoramic view of the fault.

10. The Drepanokefala - Georgioupoli Fault (fig. 22) corresponds to a group of parallel faults between Drepano Cape and Georgioupoli, of a total length of 15km, trending N-S and dipping at a high-angle to the East. The kinematic and dynamic profile of the fault coincides with the observed pattern of the other large N-S trending faults, hence it was considered to belong to the D_2 event, and characterized as possibly active.

Figure 22. Neotectonic-geological map and geological cross-section of the Drepanokefala - Georgioupoli fault zone

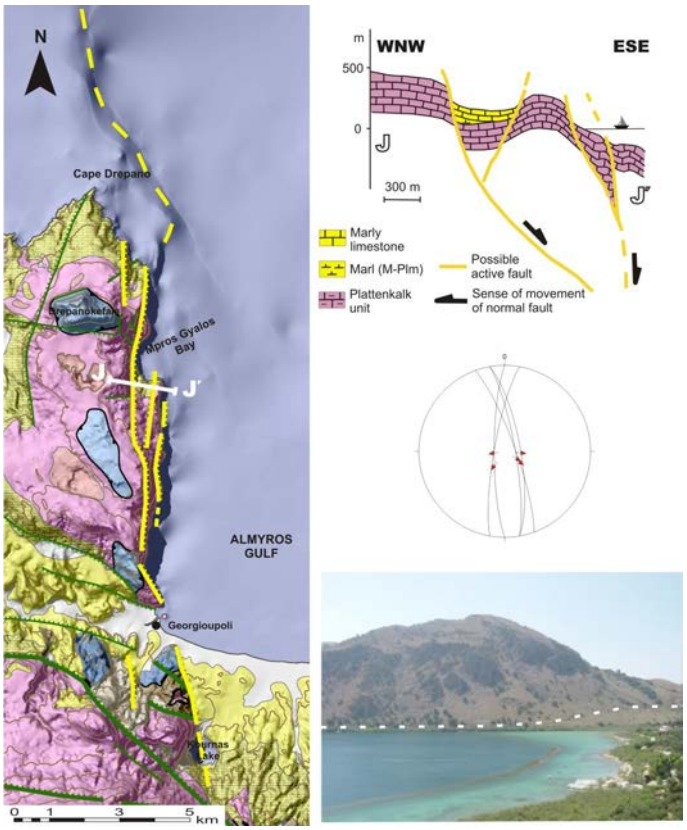

(for map legend see fig. 5). Schmidt diagram (lower hemisphere projection) showing the kinematics of Drepanokefala - Georgioupoli fault zone, compatible to D_2 event. Photo: A panoramic view of the fault, along the western coast of Kournas Lake.

11. The Fault of Argiroupoli - Kournas - Habathas (fig. 23) is a large fault zone of NW-SE strike and dipping towards the NE, acting as a boundary fault between the basement and the homonymous Neogene basin. It is composed by several spatially distributed segments, with a total length of 20km. Though the fault development is not compatible with the active stress field, two slip patterns were observed on its rupture surfaces, namely an initial ca. dip-slip one (D_1 event), followed by a second lateral to horizontal one, indicating the fault's reactivation during D_2 event of Upper Pliocene – Quaternary age.

Figure 23. Neotectonic-geological map and geological cross-section of the Argiroupoli - Kournas - Habathas fault zone

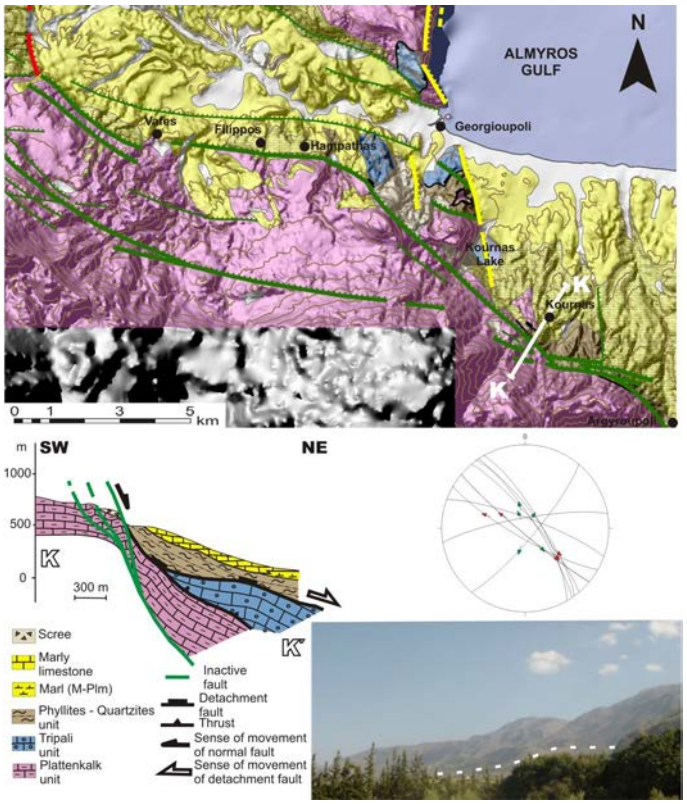

(for map legend see fig. 5). Schmidt diagram (lower hemisphere projection) showing the kinematics of the fault zone, compatible to both D_1 (green) and D_2 (red) event. Photo: A panoramic view of the fault.

12. The Fault of Zourva (fig. 24) represents a fault line of significant length, which crosses the whole western Crete (Chania) area, reaching up to the Rethymnon region. The fault is clearly observable also in satellite images, having a roughly E-W strike and a high-angle dip to the North. The fault is clearly related to the Miocene extensional detachment of the nappes, but has been also activated during both the D_1 event, with an important dip-slip component of motion towards the North, as well as during the recent D_2 event, showing an important strike-slip component and a lateral sinistral sense of shear.

Figure 24. Neotectonic-geological map and geological cross-section of the Zourva fault zone

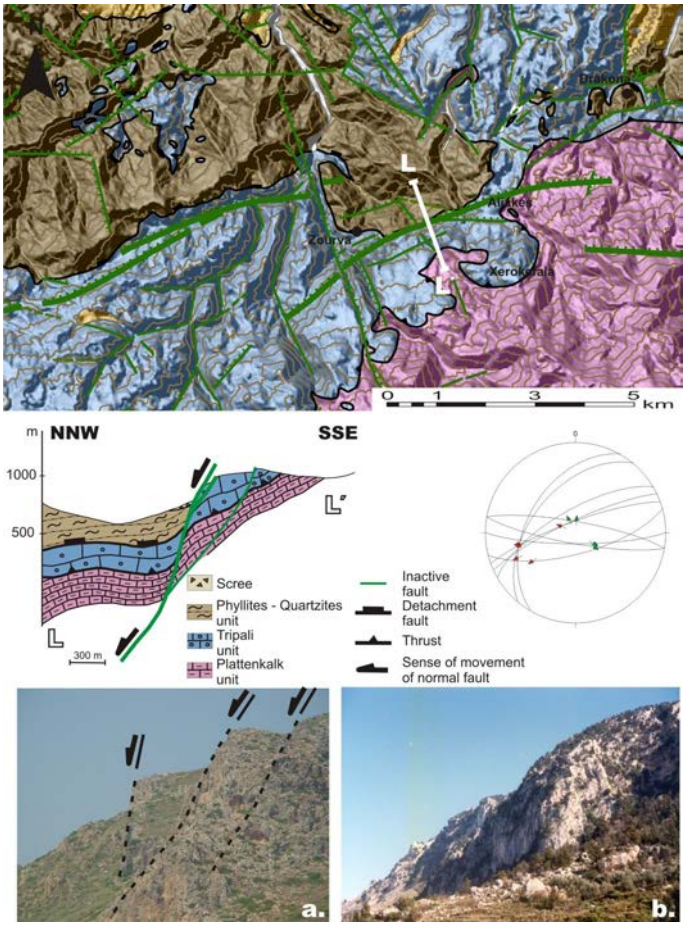

(for map legend see fig. 5). Schmidt diagram (lower hemisphere projection) showing the kinematics of the fault zone, compatible to both D_1 (green) and D_2 (red) event. Photo: a. Normal duplex structures along Zourva fault zone, b. High-angle fault plane of Zourva fault.

13. The Fault of Xiropotamos - Elos - Myloi (fig. 25) is a fault zone of NE-SW strike, dipping towards the NW. The fault is composed of three continuous segments, with a length of 8.5km, 4km and 5.5km, respectively. It mainly crosses basement rocks along the Xiropotamos stream, but also forms Pleistocene tectonic scree along its trace. The kinematics and dynamics of the fault are in accordance with the D_2 event, with a main dip-slip normal and minor horizontal sinistral component. The compatibility with the recent (active) stress field, as well as the presence of small magnitude seismicity along the fault line, suggest that this fault can also be characterized as possible active.

Figure 25. Neotectonic-geological map and geological cross-section of the Xiropotamos - Elos - Myloi fault zone

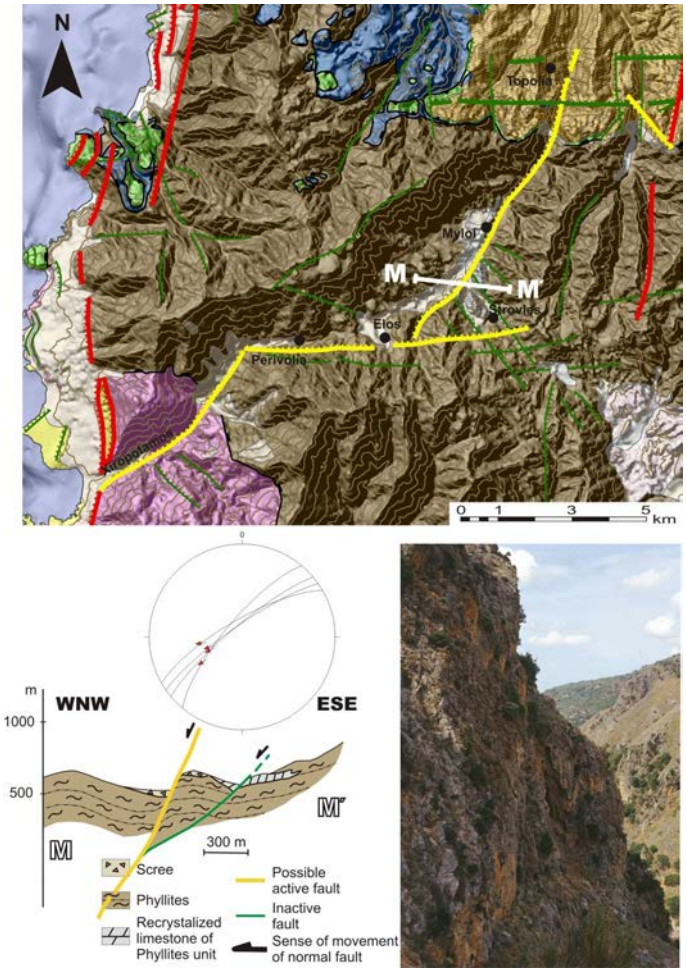

(for map legend see fig. 5). Schmidt diagram (lower hemisphere projection) showing the kinematics of the fault zone, compatible to D_2 event. Photo: A fault plane of a segment of Xiropotamos - Elos - Myloi fault zone with an impressive cataclastite.

Correlation of the faults with the fault plane solutions

In order to further explore the possible correlation of the mapped faults with the fault plane solution data, we have grouped all fault plane solution data in an elliptical region around each of the previous 13 main faults and computed average fault plane solutions using the method of Papazachos and Kiratzi (1992). The same approach has been adopted for the neotectonic information, wherever this was possible. The results are shown in Figure 26, where we present both earthquake and neotectonic information as equivalent fault plane solutions for three faults or groups of faults (1: Western Crete, 2-3: Malathiros - Rodopos/Kera-Karthiana and 12: Zourva), when this estimation was possible. Unfortunately, for the mapped faults in the eastern part of the study area (which exhibits much lower seismicity levels) it was not possible to have results from earthquake fault plane solutions. For both average mechanisms depicted in fig. 26, the main fault plane is identified with a thick line. The selection of this fault plane was obvious for the neotectonic observations (determined from field work), while for the earthquake data we simply adopted the fault plane that best correlated with the equivalent neotectonic fault plane solution and the mapped active fault orientation.

Figure 26. Average fault plane solutions

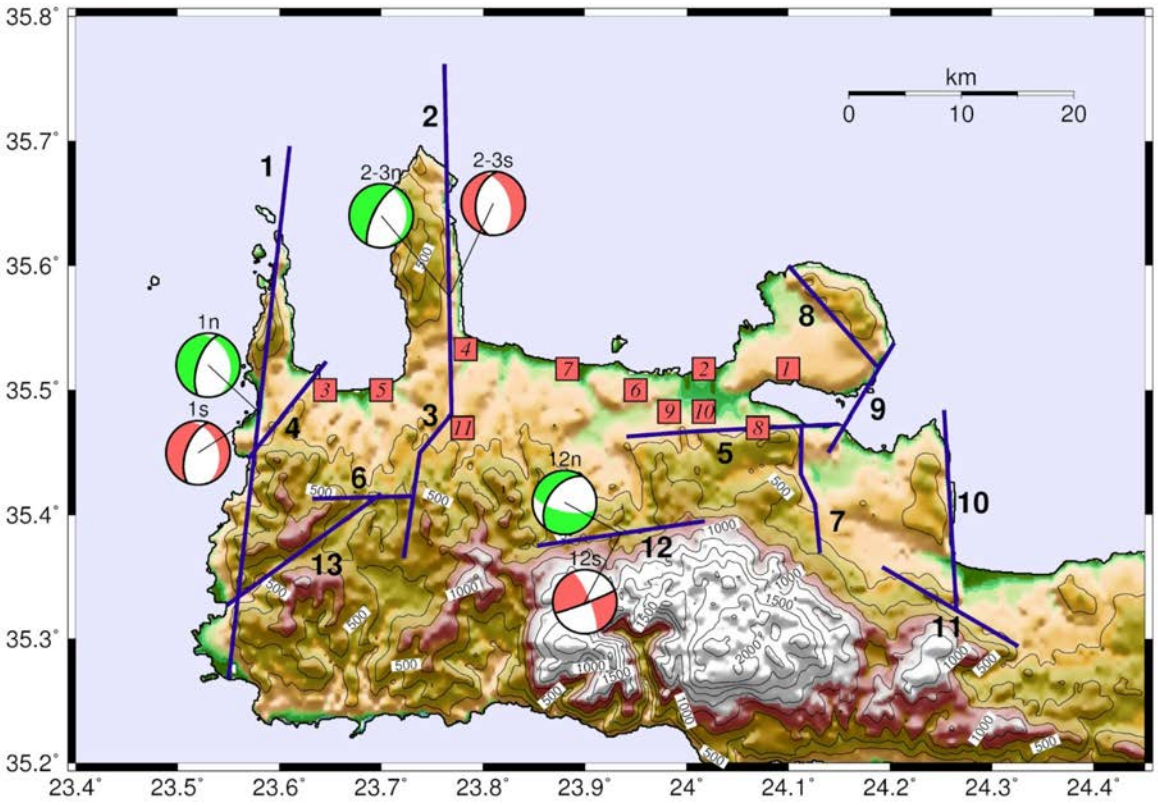

Average fault plane solutions computed using the method of Papazachos and Kiratzi (1992) for faults 1 (Western Crete), 2-3 (Malathiros - Rodopos and Kera-Karthiana) and 12 (Zourva), from the available earthquake fault plane solution data (pink colored average solutions), as well as the corresponding neotectonic information from field observations (green colored average solutions). The main fault-plane is depicted with a thick line (see text for explanations). Red squares correspond to selected sites (former municipality centers) for which seismic hazard analysis was performed (1:Akrotiri, 2: Chania, 3: Kissamos, 4: Kolymvari, 5: Mythimna, 6: N.Kydonia, 7: Platanias, 8: Souda, 9, Therissos, 10: Venizelos, 11: Voukolies)

The results verify the good to excellent agreement of neotectonic and earthquake information, even at a quite local (fault) scale. For the major N-S normal faults (1, 2-3), both solutions indicate a clear E-W extension, with a dip to the West. Even more surprisingly, the Zourva fault (12), which is not optimally oriented with respect to the active stress-field, operates as a sinistal strike-slip fault, with the earthquake information being more compatible with the strike of the observed (mapped in the field) fault trace. These results verify the reliability of the active fault mapping and of the corresponding determined younger extensional phase (D_2), as well as the proposed reactivation of older E-W trending faults as strike-slip faults under the recent E-W extensional regime.

Determination of active faults: Seismic potential and seismic hazard assessment

Using the fault information previously presented, as well as the currently accepted criteria, also adopted by the Greek Earthquake Planning and Protection Organization, the previously described faults were distinguished as active, possible active and geological (not active) (fig. 5, 7; for explanation see the detailed description of each fault zone 1-13). Following this separation, their seismic potential was assessed for the active and possible active faults, on the basis of the relation logL = 0.51*M-1.85 (Papazachos, 1989), relating the moment magnitude, M, of the maximum expected earthquake with the total length, L, of the fault. Following this approach, the following categorization was performed:

Active faults

- The fault of Western Crete, with a total length of 65km and a maximum expected earthquake magnitude M = 7.2. However, the fault is displaying a clear spatial segmentation, which most probably suggests its segmented activation with typical events of M = 5.6 to 5.7 according to the partly length of the segments. The fault is characterized as active by both neotectonic and seismological criteria.

- The fault of Malathyros - Rodopos, which is characterized active on the basis of geological and seismological criteria. Its total length of ~30km, corresponds to a maximum expected earthquake of M = 6.5. On the other hand, according to its spatial segmentation, a M = 5.5 event is the possible magnitude expected for its southern segment, while a M = 6.1 earthquake should be considered for the northern one.

- The fault of Kera - Karthiana, characterized as active by geological and seismological criteria, with a maximum magnitude M = 5.0.

- The fault of Platanos, considered as active on the basis of geological criteria. Total length ~10km corresponds to a maximum magnitude M = 5.6, with its sub-segments resulting of M = 5.2 and 4.8.

- The fault of Zacharias - Pomonia, described as active using geological criteria, with a total length of ~11km, resulting in a maximum magnitude of M = 5.7.

- The fault of Marathi, determined as active on the basis of geological criteria, with a total length ~12km and a maximum magnitude M = 5.7.

Possibly active faults

- The fault of Xiropotamos - Elos - Myloi, which is described as possibly active, mainly considering the available seismological data and geometric criteria. The expected earthquake magnitudes for its two separate segments are M = 5.1 and 5.5, respectively.

- The fault of Malaxa - Souda, characterized as possibly active mainly using geometric, kinematic and morphotectonic criteria. Its total length of ~22km corresponds to a, maximum magnitude of M = 6.2, though no historical information on similar magnitude strong earthquakes exist for this fault.

- The fault of Drepanokefala - Georgioupoli, determined as possibly active on the basis of geological and morphotectonic criteria. It has a total length of ~12.5km, corresponding to a maximum magnitude of M = 5.8.

The previous information was used in order to perform a quantitative assessment of seismic hazard for the broader W.Crete study area. For this reason we considered the previously described active and possibly active faults, as well as the general seismotectonic setting of the broader area, depicted in Fig. (10). As a first step, we used all the available historical and instrumental seismicity information for the broader western Crete area, in order to assign appropriate quantitative seismicity measures to the previously described active faults, as well as to major faults of the broader area (e.g. Elafonissos fault, fig. 1) affecting the study area.

For the historical seismicity information we mostly relied on the catalogue of Papazachos and Papazachou (2003), whereas instrumental seismicity information was based on the catalogue of the Geoph. Lab. of the Aristotle Univ. of Thessaloniki (http://seismology.geo.auth.gr/ss/CATALOGS/seiscat.dat) which reports original or converted (equivalent) moment magnitudes for all events up to 2009. Figures (27a) and (27b) present the distribution of the corresponding shallow ($h < 60$km) and intermediate-depth ($h > 60$km) earthquakes for the broader study area. These maps show that the northern part of Crete island exhibits relatively low and smaller magnitude seismicity levels, whereas larger magnitude events ($M \geq 6.0$) are observed mainly along the outer Hellenic arc, clearly related with the convergence of the Eastern Mediterranean with the Aegean plate. An exception is the Western Crete fault area, that shows relatively higher seismicity levels that the remaining western Crete mainland. On the other hand, the intermediate-depth events are distributed along a well-defined Benioff zone with amphitheatrical shape (see also fig. 1), dipping towards the Aegean sea area (Papazachos and Comninakis, 1971).

Figure 27. Spatial distribution

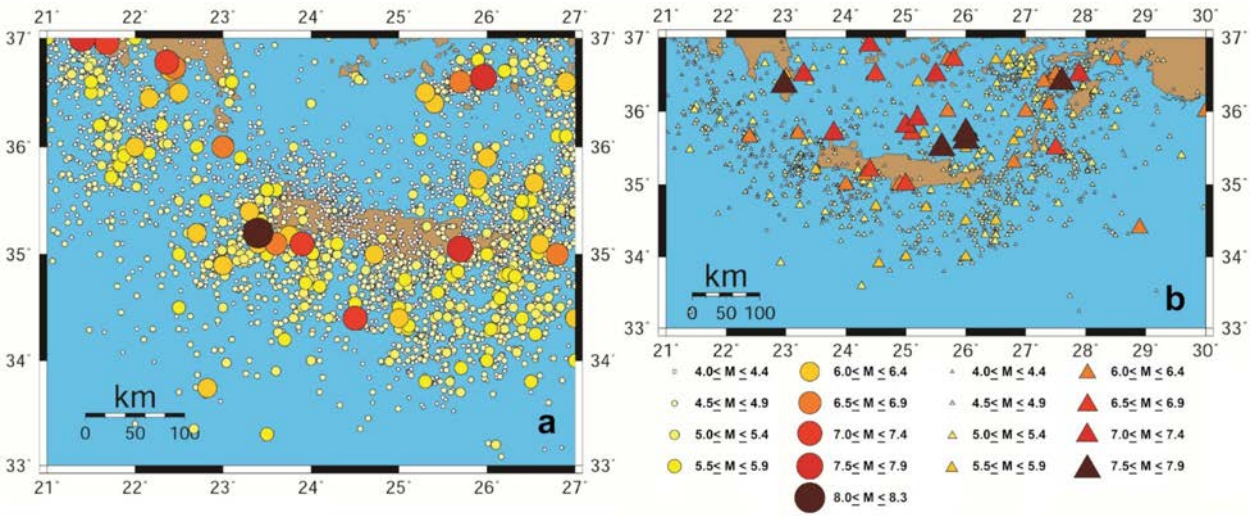

Spatial distribution of the (a) shallow (h < 60km) and, (b) intermediate-depth (h > 60km) earthquakes for the broader Western Crete area used in the present work.

The available seismological information was used to determine the catalogue completeness from the Gutenberg-Richter curve and plots of the cumulative number of earthquakes versus time for several minimum magnitudes. The finally determined completeness for the western Crete area was defined as: 1981-2002 $M \geq 3.5$; 1964-2002 $M \geq 4.0$; 1950-2002 $M \geq 4.5$. Using this completeness and the available neotectonic and seismological information, we estimated appropriate seismicity parameters using elliptical areas around each of the 13 previously examined faults. Typical Gutenberg-Richter distributions for Western Crete and Zourva faults are presented in fig. (28). Furthermore, besides the mostly normal neotectonic faults studied here, we also considered the major thrust faults in the NE-SW compression area (orange region in Fig. 10), where large magnitude events are observed. The most typical example, which strongly influences the seismic hazard assessment in the broader western Crete area, is the major Elafonisos fault that generated the 365BC M = 8.3 event (e.g. Papazachos, 1990), depicted in Fig.1. Using the same seismicity catalogue and completeness, we also estimated the corresponding seismicity parameters for this fault. It should be noted that for all other areas outside the examined western Crete neotectonic faults and the Elafonisos thrust fault, as well as for intermediate-depth events (h > 60km) we adopted the seismicity parameters of the zonation model proposed by Papaioannou and Papazachos (2000).

Figure 28. Gutenberg-Richter frequency-magnitude distributions for the Western Crete (left) and Zourva (right) faults

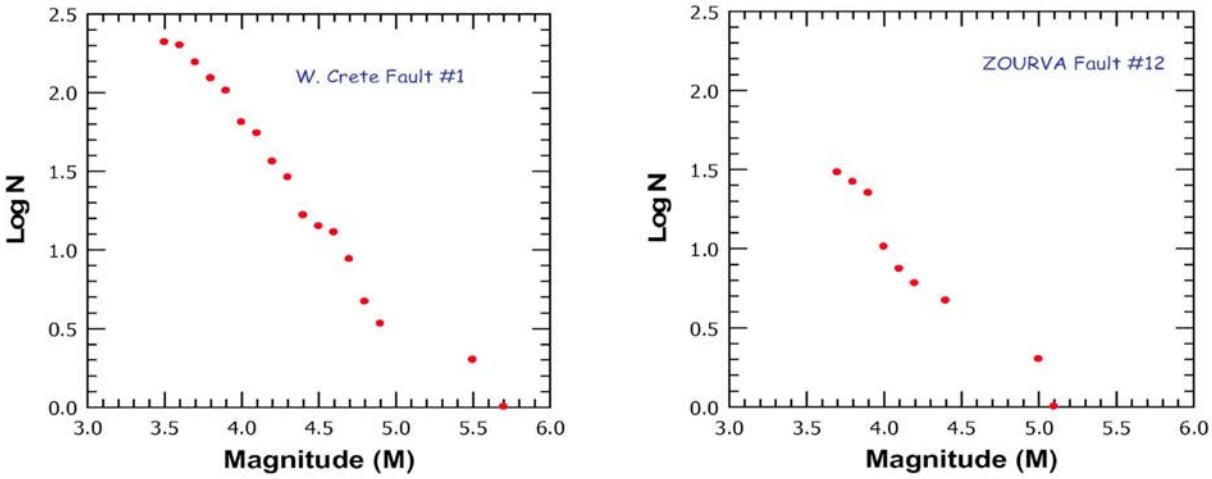

(shown in fig. 26)

In order to perform the final seismic hazard estimations we employed the PGA attenuation relation of Margaris *et al.*, (2001) for shallow earthquakes and the relations of Theodulidis and Papazachos (1990) for intermediate-depth events, which have been defined for the broader Aegean area. Seismic hazard estimations were performed using the Frisk88M (1995) code, appropriately modified in order to account for the different attenuation relations between shallow and intermediate-depth events, as well as anisotropic radiation of seismic energy at the source (Margaris, 1994). Moreover, pseudo-velocity response spectra PSV(T) (in cm/sec) were also computed using the relations of Theodulidis and Papazachos (1994).

Estimations were performed for 11 selected major sites, corresponding to the centers of the former Kapodistrian municipalities, presented with squares in fig. 13. Seismic hazard results were estimated for a 10% probability exceedence in 50 yr or equivalently for a return period of 476 yr. Typical results are presented in fig. 29, for 4 selected sites (Akrotiri-1, Chania-2, Kolymvari-4, Kissamos-3, numbering follows the sequence numbers presented in fig. 26). The sites have been selected in order to observe the gradual variation of the obtained seismic hazard results, as we move from the eastern (lower seismicity) to the westernmost (higher seismicity) part of the examined area. The presented results clearly show higher seismic hazard levels for the Kissamos site, as it is affected by the presence and related seismicity of the major neighboring Western Crete fault. On the other hand, the Kolymvari site exhibits quite low seismic hazard levels, despite being close to the neighboring active faults (Malathyro-Rodopos and Kera-Karthiana faults, numbered 2 and 3 in fig. 26). The results exhibit an important spatial variability of seismic hazard, despite the small spatial extent of the study area, suggesting that the identified active faults have an important effect on the seismic hazard assessment.

Figure 29. Seismic hazard curves for the former municipalities of Akrotiri, Chania, Kolymvari and Kissamos

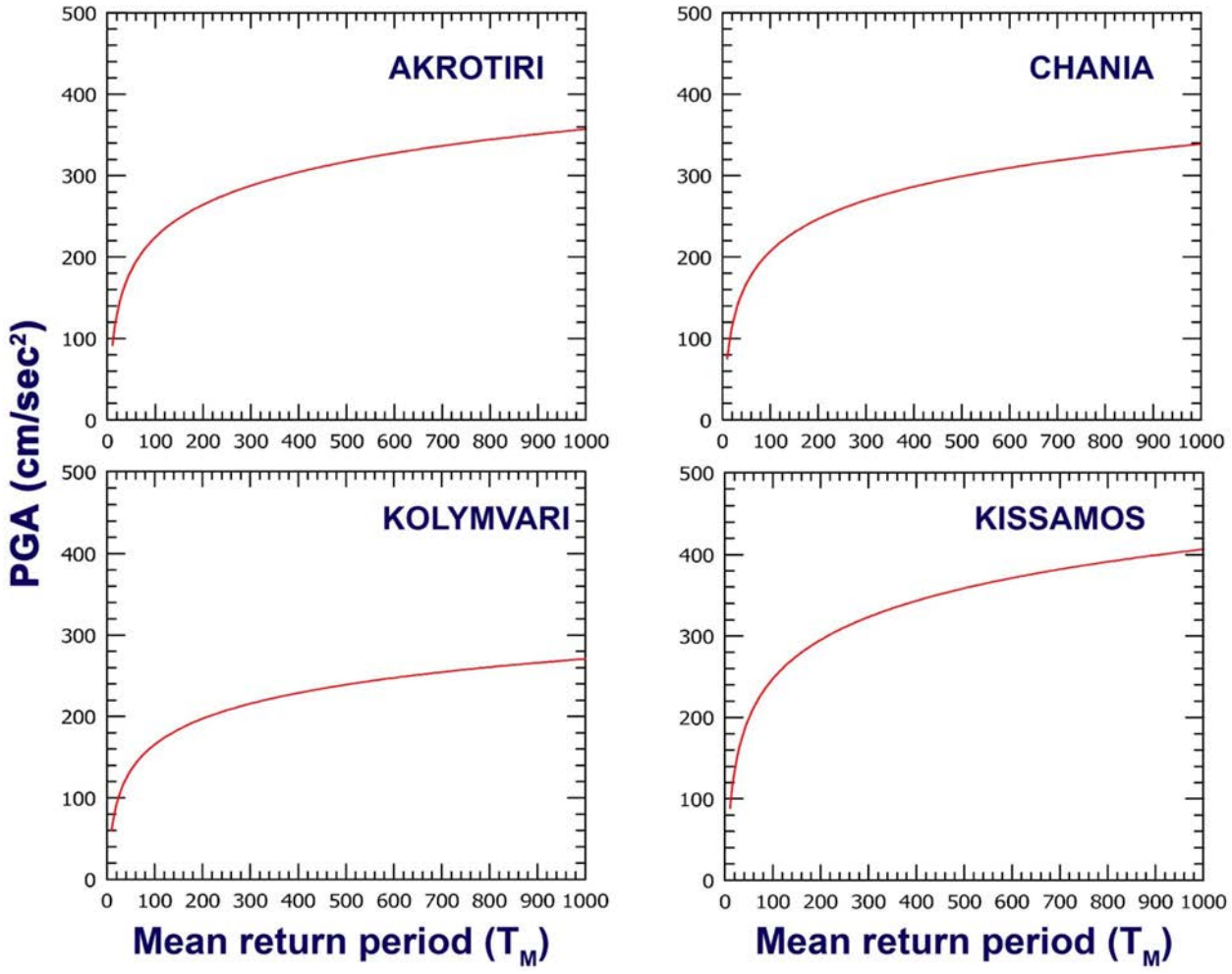

(see fig. 26 for locations).

In order to further explore this issue and propose appropriate design spectra, we followed a specific approach in order to quantify the effect of the seismotectonic model on the seismic hazard assessment. For this reason appropriate deaggregation of the seismic hazard results was performed for each examined site and all seismic sources (e.g. neotectonic faults, Elafonissos thrust fault, intermediate-depth event zones, etc.) affecting this site. The corresponding earthquake scenario were considered as design earthquakes and used in a stochastic simulation procedure, in order to estimate the contribution of each fault on the seismic hazard of each site.

For the stochastic simulation we employed the methodology of Beresnev and Atkinson (1997), which extends the original method of Boore (1983) by considering the finite seismic source dimensions. This modification is especially important for the near source strong motion effects and has been widely employed for several seismotectonic environments. The method assumes a planar fault surface, divided into smaller segments, where each segment can be considered as an independent Brune point source. The seismic rupture propagates from a starting nucleation point using a constant rupture velocity and the final seismic wavefield is computed by the summation of the contribution of each segment by incorporating appropriate geometrical and anelastic attenuation, as well as empirical site-effects (Beresnev and Atkinson, 1997, 1998, 1999, 2001a,b).

Using the stochastic simulation approach for the design events, as their magnitude was determined from the deaggregation analysis and their fault plane characteristics from the neotectonic and fault plane solution information, average elastic response spectra (for 5% damping and amplification factor of β_0 = 2.5) were computed

using a large number of simulations (typically 30) for each site. Sample results are presented in fig. 30 for the same sites as in fig. 29. Moreover, the probabilistic elastic response spectra as determined from the initial seismic hazard analysis for two site conditions (rock and stiff soil), as well as the Greek Seismic Code (NEAK) elastic design spectra are also presented for all sites. It should be noted that: a) The NEAK spectra are identical for all sites, as they belong to the same seismic hazard zone (elastic spectra acceleration of 0.6g), b) Since almost all examined sites are located on relatively stiff Neogene sediment deposits, the stiff soil probabilistic spectra should be considered as more appropriate for the examined sites and, c) The stochastic simulation elastic spectra correspond to the scenarios determined from the de-aggregation process and not to worst-case scenarios for each examined fault.

Figure 30. Comparison of stochastic simulation elastic response spectra

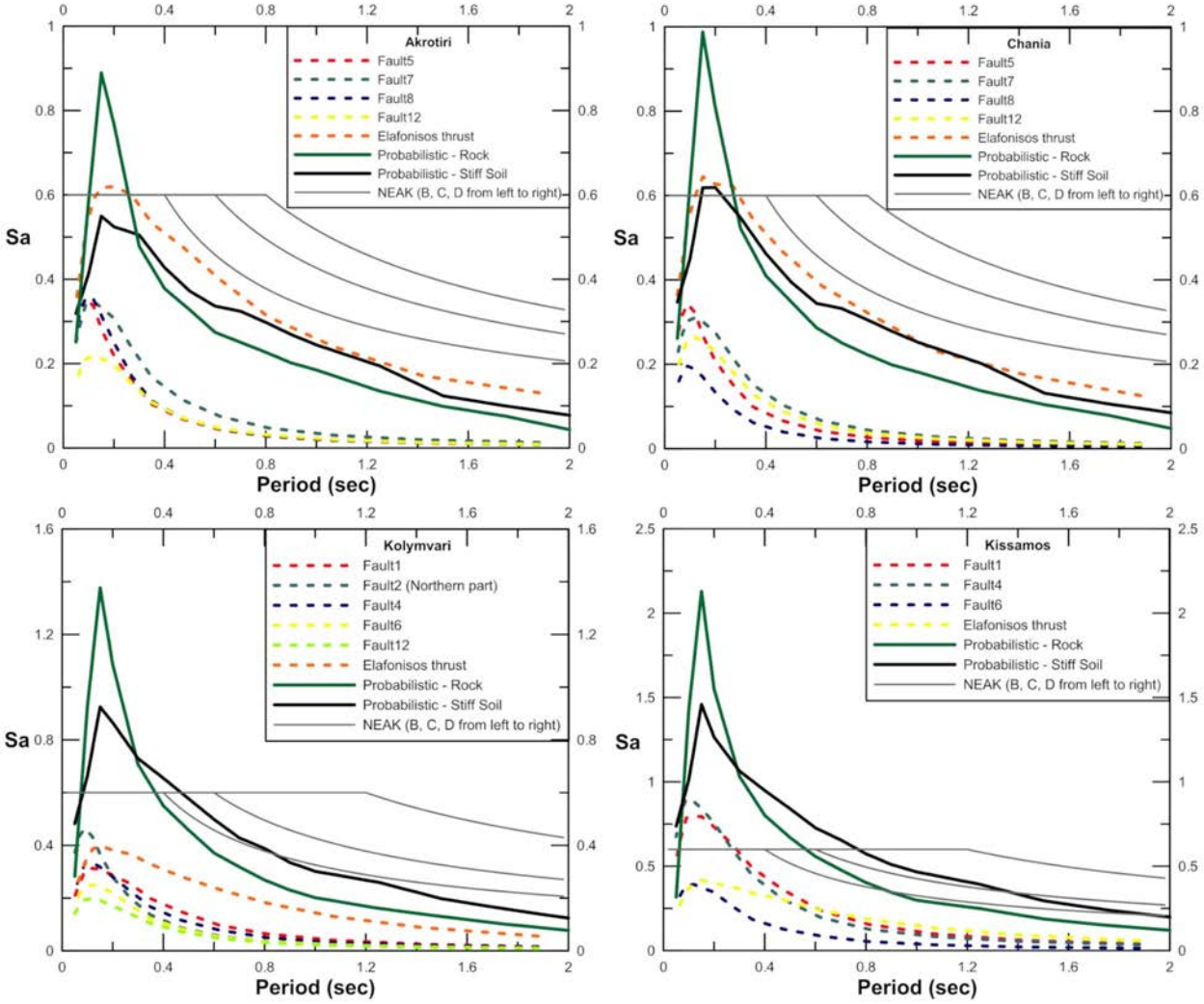

Comparison of stochastic simulation elastic response spectra from the deaggregation analysis with the corresponding probabilistic elastic spectra from seismic hazard assesment and the Greek Seismic Code (NEAK) elastic response spectra for the former municipalities of Akrotiri, Chania, Kolymvari and Kissamos (see fig. 5 for locations).

The results further confirm the strong spatial variability of the seismic hazard in the western Crete area. On the other hand, the presented results show two different pictures for the examined sites. More specifically, for sites located in the eastern (lower seismicity) part of the study area (Akrotiri, Chania) the NEAK (Greek Seismic Code) elastic response spectra cover the probabilistic estimates

from the hazard analysis. Moreover, the main contribution in seismic hazard is due to the Elafonisos thrust fault, which is almost identical to the probabilistic estimate. This observation suggests that the contribution of the active but low-seismicity neighboring neotectonic faults (faults 5, 7, 8, etc.) is minimal and that the main source of seismic hazard for these sites is the large thrust events that originate from the outer Hellenic arc convergence zone (fig. 1).

A quite different situation holds for sites located in the western part of the study area. More specifically, compared to the Seismic Code design spectra, the probabilistic elastic spectra estimated in this study are slightly larger (up to 0.9g) at higher frequencies (2-10Hz) for Kolymvari and much larger (up to 1.45g) for a much larger frequency range (1.2-20Hz) for the Kissamos site, suggesting that the Seismic Code spectra probably need adapting, especially for the Kissamos site. Even more important is the pattern change regarding the seismic hazard source contributions: For the Kolymvari site the contribution of the Elafonisos thrust fault is comparable to the contribution of the neighboring active normal faults, mainly the Malathyros-Rodopos fault (fault 2), especially for higher frequencies (lower periods). This pattern is even more enhanced for the Kissamos site, where the neighboring fault group (Western Crete-fault 1 and Platanos-fault 4), which exhibits higher seismicity levels, control the seismic hazard, while the Hellenic arc thrust fault contribution is significantly smaller. This result further verifies the importance for the detailed neotectonic mapping for seismic hazard assessment, especially at the local scale level performed in the present work.

Discussion-Conclusions

The detailed neotectonic study and complementary seismotectonic analysis show a compatible, almost identical picture of the ongoing active processes that control the normal fault generation on Western Crete, which corresponds to the southwesternmost part of the Hellenic Arc area. After the neotectonic analysis we conclude that two distinctive stress phases took place since Middle Miocene to present. The first one (D_1, Mid-Upper Miocene to Lower Pliocene) exhibits a N-S extension and was responsible for the formation of the dominant E-W trending normal faults that control the shape of the large Neogene basins of Western Crete. The second one (D_2, Lower Pliocene to present) exhibits a E-W extension, forming mainly N-S faults, but also NE-SW trending smaller faults with significant strike-slip component, often acting as transfer zones between the larger N-S fault zones. Moreover, some large E-W faults from the previous D_1 phase are often re-activated, during the later D_2 phase, as almost pure strike-slip faults. Neotectonic and seismotectonic fabric is strongly controlled by the dynamics of N-NNE-ward subduction processes of the African plate under the Crete island which belongs to the forearc area of the Hellenic island arc.

This pattern is in excellent agreement with the seismological information, that show mostly N-S normal fault mechanisms, as well as NW-SE and NE-SW strike-slip mechanisms with significant normal component. Moreover, the determined active stress field from fault plane solution data also shows a dominant E-W extension, suggesting that the later D_2 phase identified by field fault data is an on-going active process.

The neotectonic information was jointly evaluated together with the available seismological data in order to create a more complete picture about the seismic hazard of the study area. Using a combination of field data and seismicity information, 13 large major fault zones were defined and studied for the area, with nine of them characterized as active or possible active faults. These nine faults were incorporated in a detailed seismic hazard analysis, which also took into account the large thrust fault zones of the outer Hellenic arc, as well as the Benioff-zone intermediate-depth events.

The combination of both a probabilistic and a deterministic approach for seismic hazard evaluation, allowed not only the reliable estimation of the seismic hazard for several selected sites but also the effective de-aggregation of the seismic hazard results. The obtained hazard estimates show a significant spatial variation of seismic hazard, mainly due to the different effect of the studied faults on each site. Furthermore, the role of the on-land, mainly normal, active faults, in comparison to the large thrust fault of the outer Hellenic arc varies significantly. More precisely, the seismic hazard of the westernmost part of study area is mainly controlled by the neighboring higher seismicity neotectonic faults, while the corresponding hazard of the central and easternmost part is mostly affected by the large outer arc thrust faults (e.g. Elafonisos fault). These results suggest that this combined interpretation of field (neotectonic) data with seismological information is essential, not only for the better

understanding of the ongoing seismotectonic processes but also for the efficient and reliable estimation of seismic hazard and the corresponding probabilistic or deterministic analysis.

References

Angelier J. (1979). Determination of the mean principal directions of stresses for a given fault population. Tectonophysics, 56, T17-T26.

Angelier J., Tarantola A., Valette B. and Manoussis S. (1982). Inversion of field data in fault tectonics to obtain the regional stress. Part I. Simple phase fault populations: a new method of computing the stress tensor. Geophys. J., R. Astr. Soc., 6, 607-621.

Armijo R., Lyon-Caen H. and Papanastasiou D. (1992). East-west extension and Holocene normal-fault scarps in the Hellenic arc. Geology, 20, 491-494.

Beneke K., Schwarte J. and Peterek A. (2002). Quartave Hebungs – und Bewegurigs raten au Westrand der Insel Krete – abgeleited aus, morphotektonischen Untersuchungen. Grlanger Geologische Abhandlungen, TSK9, 9 (Abstract).

Beresnev I.A. and Atkinson G.M. (1997). Modeling finite-fault radiation from the ωn spectrum. Bull. Seism. Soc. Am., 87, 67-84.

Beresnev I.A. and Atkinson G.M. (1998). FINSIM – a FORTRAN program for simulating stochastic acceleration time histories from finite faults. Seism. Res. Lett., 69, 27-32.

Beresnev I.A. and Atkinson G.M. (1999). Generic finite-fault model for ground-motion prediction in eastern North America. Bull. Seism. Soc. Am., 89, 608-625.

Beresnev I. and Atkinson G. (2001)a. Subevent structure of large earthquakes – A ground motion perspective. Geophys. Res. Lett., 28, 53-56.

Beresnev I. and Atkinson G. (2001)b. Correction to "Subevent structure of large earthquakes – A ground motion perspective". Geophys. Res. Lett., 28, 4663.

Besnard M. (1991). Sismotectonique de l'arc egeen, resultants d'une campange de microsismicite. PhD. Thesis, Grenoble, France.

Bonneau M. (1976): Esquisee structurale de la Crete alpine. Bul. Soc. Geol. France, 18, 351-353.

Bonneau M. (1984). Correlation of the Hellenic nappes in the southern Aegean and their tectonic reconstruction. In the Geological Evolution of Eastern Mediterranean, ed. J.E. Dixon, A.H.F. Robertson, Geol. Soc. London, Spec. Publ., 17, 517-527.

Boore D.M. (1983). Stochastic simulation of high-frequency ground motions based on seismological models of the radiated spectra. Bull. Seism. Soc. Am., 73, 1865-1894.

Chabalier B.J., Lyon-Caen H., Zollo A., Deschamps A., Bernard P and Hatzfeld D. (1992). A detailed analysis of microearthquakes in western Crete from digital three-component seismograms. Geophys. J. Int., 110, 347-360.

Creutzburg N. and Seidel E. (1975). Zum Stand der Geologie des praeneogens auf Kreta. N. Jahrb. Geol. Palaeont. Abh., 149, 363-383.

Duevmeijer C.E., Krijgsman W., Langereis C.G. and ten Veen J.H. (1998). Post-early Messinian counterclockwise rotation on Crete: implications for Late Miocene to recent kinematics of the southern Hellenic arc. Tectonophysics, 298, 177-189.

Duyster J. (2000). Stereo Nett. Microsoft Corp., Universtität Bochum.

Fassoulas C., Kilias A. and Mountrakis D. (1994). Postnappe stacking extension and exhumation of high-pressure/low temperature rocks in the island of Crete, Greece. Tectonics, 13, 127-138.

Freudenthal T. (1969). Stratigraphy of Neogen deposits in the Chania province Crete, with special reference to foraminifera of the family planorbulinidae and the genus Heterostegina. Ultrecht Micropal. Bull., 1, 1-208.

FRisk88M (1995). User's Manual, ver. 1.70. Risk Engineering Inc., Boulder Co., 69pp, 2 Appendixes.

Frydas D. and Keupp H. (1996). Biostratigraphical results in Late Neogene deposits of NW Crete, Greece, based on calcareous nannofossils. Berliner Geowiss. Abh., E18, 169-189.

Fytikas M., Innocenti F., Manetti P., Peccerillo A., Mazzuoli R. and Villari L. (1984). Tertiary to Quaternary evolution of volcanism in the Aegean region. Geological Society, London, Special Publications, 17, 687-699. 10.1144/ GSL.SP.1984.017.01.55

Gephart J.W. and Forsyth D.W. (1984). An improved method for determining the regional stress tensor using earthquake focal mechanism data: Application to the San Fernando earthquake sequence. J. Geophys. Res., 89, 9305-9320.

Goldworthy M., Jackson J. and Haines J. (2002). The continuity of active fault systems in Greece. Geophys. J. Int., 148, 596-618.

Hancock P.L. (1985). Brittle microtectonics: principles and practice. J. Struct. Geol., 7, 437-457.

Hatzfeld D., Besnard M., Makropoulos K. and Hatzidimitriou P. (1993). Microearthquake seismicity and fault plane solutions in the southern Aegean and its geodynamic implications. Geophys. J. Int., 115, 799-818.

Jolivet L., Goffe B., Monie P., Truffert-Luxey C. and Bonneau M. (1996). Miocene detachment in Crete and exhumation P-T-t paths of high-pressure metamorphic rocks. Tectonics, 15, 1129-1153.

Jost L.M., Knabenbauer O., Cheng J. and Harjes H.P. (2002). Fault plane solutions of microearthquakes and small events in the Hellenic arc. Tectonophysics, 356, 87-114.

Karagianni E.E., Papazachos C.B., Panagiotopoulos D.G., Suhadolc P., Vuan A. and Panza G.F. (2005). Shear velocity structure in the Aegean area obtained by inversion of Rayleigh waves. Geophys. J. Int., 160, 127-143.

Kilias A., Fassoulas C. and Mountrakis D. (1994). Tertiary extension of continental crust and uplift of Psiloritis metamorphic core complex in the central part of the Hellenic Arc (Crete, Greece). Geol. Rundsch., 83, 417-430.

Kilias A., Tranos M., Orozco M., Alonso-Chaves F. and Soto J. (2002). Extensional collapse of the Hellenides: A review. Rev. Soc. Geol. Espania, 15, 129-139.

Kilias A, Frisch W., Avgerinas A., Dunkl I., Falalakis G. and Ganlick H.J. (2010). Alpine architecture and kinematics of deformation of the Northern Pelagonian nappe pile in the Hellenides. Austrian J. of Earth Sciences, 103, 4-28.

LePichon X. and Angelier J. (1979). The Hellenic arc and trench system: a key to the neotectonic evolution of the eastern Mediterranean area. Tectonophysics, 60, 1-42.

Liotier Y. (1989). Modelisation des ondes de volume des seismes de l'arc Ageen. DEA de l'Universite Joseph Fourier, Grenoble, France.

Lister G.S., Banga G. and Feenstra (1984). Metamorphiccore complexes of cordilleran type in the Cyclades, Aegean Sea, Greece. Geology, 12, 221-225.

Louvari E. (2000). Detailed seismotectonic study of the Aegean and neighboring areas, using the fault plane solutions from small-magnitude events. PhD Thesis, Aristotle Univ. of Thessaloniki, Greece, pp.373.

Lyon-Caen H., Armijio R., Drakopoulos I., Baskoutas, J., Delibassis N., Gaulon R., Kouskouna V., Latoussakis J., Makropoulos K., Papadimitriou P., Papanastassiou D. and G. Pedotti (1988). The 1986 Kalamata (south Peloponnesus) Earthquake: Detailed study of a normal fault, evidences for East-West extension in the Hellenic Arc. J. Geoph. Res., 93, 14967-15000.

Margaris B.N. (1994). Azimuthal dependence of seismic wave propagation in the Hellenic area and its effect on seismic hazard. Ph.D. Thesis, Aristotle Univ. of Thessaloniki, 324pp.

Margaris B., Papazachos C., Papaioannou C., Theodulidis N., Kalogeras I. and Skarlatoudis A. (2001). Empirical attenuation relations for strong horizontal seismic motion of shallow earthquakes in Greece. Proc. 2nd Hell. Congress of Earthq. Engin. and Eng. Seismology, Vol.1, 27-36.

McClusky S., Barka A., Demir C., Ergintav S., Georgiev I., Gurkan O., Hamburger M., Hurst K., Kahle H., Kastens K., Kekelidze G., King R., Kotzev V., Lenk O., Mahmoud S., Mishin A., Nadariya M., Ouzounis A., Paradissis D., Peter Y., Prilepin M., Reilinger R., Sanli I., Seeger H. and Balassanian S. (2000). Global Positioning System constraints on plate kinematics and dynamics in the eastern Mediterranean and Caucasus. J. Geophys. Res., 105, 5695-5719, 10.1029/1996JB900351

McKenzie D.P. (1970). The plate tectonics of the Mediterranean region. Nature, 226, 239-243.

McKenzie D. (1972). Active tectonics of the Mediterranean region. Geophys. J.R. astr. Soc., 30, 109-185.

Meulenkamp J.E., van der Zwaan G.J. and van Wamel W.A. (1994). On Late Miocene to recent vertical motions in the Cretan segment of the Hellenic arc. Tectonophysics, 234, 53-72.

Mountrakis D. (2006). Tertiary and Quaternary tectonics of Greece. Geol. Soc. Amer. Bull. sp. paper 409, 125-136.

Mountrakis D., Tranos M., Papazachos C., Thomaidou E., Karagianni E. and Vamvakaris D. (2006). Neotectonic and seismological data concerning major active faults, and the stress regimes of Northern Greece. In: ROBERTSON, A. H. F. & MOUNTRAKIS, D. (eds). Tectonic Development of the Eastern Mediterranean Region. Geological Society, London, Special Publications, 260, 649-670.

Oral M.B., Reilinger R.E., Toksoz M.N., King R.W., Barka A.A., Kiniki J. and Lenk D. (1995). Global Positioning System offers evidence of plate motions in eastern Mediterranean. EOS, 76, 9-11.

Papaioannou Ch.A. and Papazachos B.C. (2000). Time-independent and time-dependent seismic hazard in Greece based on seismogenic sources. Bull. Seism. Soc. Am., 90, 22-33.

Papazachos B.C. (1989). A time predictable model for earthquake generation in Greece. Bull. Seism. Soc. Am., 79, 77-84.

Papazachos B.C. (1990). Seismicity of the Aegean and surrounding area. Tectonophysics, 178, 287-308.

Papazachos B.C. and Comninakis P.E. (1970). Geophysical features of the Greek Island Arc and Eastern Mediterranean Ridge. Com. Ren. des Seances de la Conference Reunie a Madrid, 1969, 16, 74-75.

Papazachos B.C. and Comninakis P.E. (1971). Geophysical and tectonic features of the Aegean arc. J. Geophys. Res., 76, 8517-8533.

Papazachos B.C., Papadimitriou E.E., Kiratzi A.A., Papazachos C.B. and Louvari E.K. (1998). Fault plane solutions in the Aegean sea and the surrounding area and their tectonic implications. Bolletino di Geofisica Teorica ed Applicata, 39, 199-218.

Papazachos B.C., Karakostas V.G., Papazachos C.B. and Scordilis E.M. (2000). The geometry of the Wadati-Benioff zone and lithospheric kinematics in the Hellenic arc. Tectonophysics, 319, 275-300.

Papazachos B.C., Mountrakis D.M., Papazachos C.B., Tranos M.D., Karakaisis G.F. and Savvaidis A.S. (2001). The faults which have caused the known major earthquakes in Greece and surrounding area between the 5th century BC and today. Proc. 2nd Hell. Congress of Earthq. Engin. and Eng. Seismology, Vol.1, 55-64.

Papazachos B.C. and Papazachou C.B. (2003). The earthquakes of Greece, 3rd Edition. Ziti Publ. Thessaloniki, Greece, 273pp.

Papazachos C.B. (1999). Seismological and GPS evidence for the Aegean-Anatolia interaction. Geophys. Res. Lett., 17, 2653-2656.

Papazachos C.B. and Kiratzi A.A. (1992). A formulation for reliable estimation of active crustal deformation and its application to central Greece. Geophys. J. Int., 111, 424-432.

Papazachos C.B., Kiratzi A.A. and Papazachos B.C. (1992). Rates of active crustal deformation in the Aegean and surrounding area. Journal of Geodynamics, 16, 147 -179.

Papazachos C.B. and Kiratzi A.A. (1996). A detailed study of the active crustal deformation in the Aegean and surrounding area. Tectonophysics, 253, 129-153.

Petereck A. and Schwarze J. (2004). Architecture and Late Pliocene to recent evolution of outer-arc basins of the Hellenic subduction zone (south-central Crete, Greece). J. of Geodynamics, 38, 19-55.

Reilinger R.E., McClusky S.C., Oral M.B., King R.W., Toksoz M.N., Barka A.A., Kinik I., Lenk O., Sanli I. (1997). Global positioning system measurements of present-day crustal movements in the Arabia-Africa-Eurasia plate collision zone. J. Geophys. Res., 102, 9983-9999.

Ring U., Glodny J., Will T. and Thomson S. (2010). The Hellenic subduction system: High-pressure, metamorphism, exhumation, normal faulting and large-scale extension. Ann. Rev. Earth Planet. Sc., 38, 45-76.

Seidel E., Kreuzer H. and Harre W. (1982). A Late Oligocene/ Early Miocene high pressure belt in the external Hellenides. Geol. Jahrb., E 23, 165-206.

Shaw B., Ambraseys N.N., England P.C., Floyd M.A., Gorman G.J., Higham T.F.G., Jackson J.A., Nocquet J.M., Pain C.C. and Piggott M.D. (2008). Eastern Mediterranean tectonics and tsunami hazard inferred from the AD 365 earthquake. Nature Geoscience, 1, 268-276.

Stiros S. (2001). The AD 365 Crete earthquake and possible seismic clustering during the fourth to sixth centuries AD in the Eastern Mediterranean: a review of historical and archaeological data. J. Struct. Geol., 23, 545-562. 10.1016/ S0191-8141(00)00118-8

Suppe J. (1985). Principles of Structural Geology. Prentice Hall. Inc., 537p.

ten Veen J.H. and Meijer P.T. (1998). Late Miocene to recent tectonic evolution of Crete (Greece): geological observation and model analysis. Tectonophysics, 298, 191-208.

ten Veen J.H. and Kleinspehn K.L. (2003). Incipient continental collision and plate-boundary curvature: Late Pliocene – Holocene transtensional Hellenic forearc, Crete, Greece. J. Geol. Soc. London, 160, 1-6.

Theodulidis N. and Papazachos B. (1990). Strong motion from intermediate depth subduction earthquakes and its comparison with that of shallow earthquakes in Greece. Proc. XXII Gen. Assembly ESC, Barcelona 1990, II, 857-864.

Theodulidis N. and Papazachos B. (1994). Dependence of strong ground motion on magnitude-distance, site geology and macroseismic intensity for shallow earthquakes in Greece: II, Peak horizontal pseudovelocity. Soil Dyn.Earth. Eng., 13, 317-343.

Turner F. (1953). Nature and dynamic interpretation of deformation lamellae in calcite of three marbles. Am. J. Sci., 4, 276-298.